Geologic and Geophysical Maps of the Eastern Three-Fourths of the Cambria 30´ x 60´ Quadrangle, Central California Coast Ranges

Pamphlet to accompany

Scientific Investigations Map 3287

2014

U.S. Department of the Interior
U.S. Geological Survey

This page is intentionally left blank

Contents

Contents ii
Introduction 1
Interactive PDF 2
Stratigraphy 5
Basement Complexes 5
Salinian Complex 5
Great Valley Complex 10
Franciscan Complex 11
Early Quaternary and Tertiary Strata 12
Piedras Blancas Block 12
Santa Lucia Range Block 12
San Antonio Block 12
Quaternary Surficial Deposits 13
Paleontology 13
Radiometric Ages 14
Geophysical Data 14
Gravity Anomalies 18
Magnetic Anomalies 19
Structure 20
Structural History 25
Description of Map Units 28
Quaternary surficial deposits 28
Early Quaternary and Tertiary strata 31
Piedras Blancas Block 31
Santa Lucia Range Block 32
San Antonio Block 34
Basement complexes 35
Salinian complex 35
Franciscan Complex 36
Cambria terrane 37
Unnamed Disrupted Terrane(s) 37
Great Valley complex 38
Great Valley Sequence 38
Coast Range ophiolite 38
References Cited 39

Figures

1. Shaded relief map of the onshore part of the Cambria 30´ x 60´ quadrangle, annotated with geographic names used in the text.....3
2. Index map of structural blocks and named faults in the map area.....4
3. Index map of tectonostratigraphic elements in the map area.....6
4. Maps and cross-sections illustrating the tectonostratigraphic setting and history of the study area.....7
5. Gravity and aeromagnetic maps of the study area.....15
6. Cross section of the map area and an adjacent area to the east, through Point Piedras Blancas and San Antonio Reservoir, with gravity and magnetic model.....21
7. Index map of microseismicity in the map area, color-coded by depth.....24

Tables

1. Specifications of aeromagnetic surveys within the Cambria quadrangle.....18

Geologic and Geophysical Maps of the Eastern Three-Fourths of the Cambria 30´ x 60´ Quadrangle, Central California Coast Ranges

By R.W.Graymer, V.E. Langenheim, M.A. Roberts, and Kristin McDougall

Introduction

This report contains geologic, gravity anomaly, and aeromagnetic anomaly maps of the eastern three-fourths of the 1:100,000-scale Cambria quadrangle and the associated geologic and geophysical databases (ArcMap databases), as well as complete descriptions of the geologic map units and the structural relations in the mapped area. A cross section is based on both the geologic map and potential-field geophysical data.

The geologic map is a significantly modified version of an unpublished geologic map compiled by V.M. Seiders in the early 1990s. Three factors led to the decision to remap the area rather than publish this existing compilation. First, almost 20 years of new geologic information has been gathered for the map area. Second, tectonic models for the California Coast Ranges have changed since the 1990s, and these new models have a strong influence on the depiction of through-going faults, volcanic fields, folds, and other mapped features. Third, areally consistent and continuous potential-field datasets make it possible to map concealed faults and rock bodies in a way that was not possible before. Changes to the Seiders geologic map include the following:

1. Updated depiction of the active San Simeon Fault Zone (considered to be part of the major Hosgri Fault Zone) and adjacent geologic map units
2. Mapping of Quaternary surficial deposits throughout the onshore map area
3. Detailed mapping in the Williams Hill area in the northeast corner of the map
4. Extensive revisions based on new mapping in the Cambria area in the southeast corner of the map
5. Revised stratigraphic depiction based on subdivision of structural blocks and Mesozoic basement terranes
6. Revised interpretations based on potential-field geophysical data.

There are also smaller additions and revisions throughout the map area.

The Cambria 30´ x 60´ quadrangle comprises southwestern Monterey County and northwestern San Luis Obispo County. The land area includes rugged mountains of the Santa Lucia Range extending from the northwest to the southeast part of the map; the southern part of the Big Sur coast in the northwest; broad marine terraces along the southwest coast; and broad

valleys, rolling hills, and modest mountains in the northeast (fig. 1). Most of the area is sparsely inhabited, including the Hunter Liggett Military Reservation, Los Padres National Forest (including a number of designated wilderness areas), and a very large tract belonging to the W.R. Hearst estate. Public roads and trails are limited, and access is therefore difficult. The unincorporated town of Cambria (population ~6,500) along the southern coast is the only sizable community. The primary point of public interest in the map area is Hearst San Simeon State Historical Monument, centered around Hearst Castle, the mega-mansion built by Julia Morgan for media magnate William Randolph Hearst on a ridge overlooking the Pacific Ocean (a ridge created by hanging-wall uplift on the active Oceanic Fault, fig. 2).

Geologic interest focused on the Cambria region in 2003, when the Oceanic Fault and related blind faults ruptured to generate the M6.6 San Simeon earthquake (a somewhat confusing name because the earthquake did not occur on the San Simeon Fault). Two lives were lost, 47 people were injured, and almost 500 homes and commercial structures were damaged in San Luis Obispo and Santa Barbara Counties (California Seismic Safety Commission, 2004). The Oceanic Fault is one of a suite of poorly understood faults that splay from the major strike-slip Hosgri Fault. We undertook regional geologic and geophysical mapping after the earthquake both to serve as a basic data set for analyses of the earthquake and associated faults and to glean insights into the fault system from the new observations.

Interactive PDF

The maps are presented as an interactive, multilayer PDF, rather than more traditional pre-formatted map-sheet PDFs. Various geologic, geophysical, paleontological, and base map elements are placed on separate layers, which allows the user to combine elements interactively to create map views beyond the traditional map sheets. For example, fault lines, traditionally part of the geologic map sheet, can be overlain on gravity data to examine the role of the faults as boundaries of bodies with differing density. A layered PDF also allows the user to select simplified views by excluding some of the elements of a traditional map sheet, such as focusing on geologic unit distribution by omitting structural data layers. In addition, a layered PDF allows the user to select either a traditional topographic map base or a topographic shaded-relief base (or no base at all). Four traditional map sheets (geologic map, gravity map, aeromagnetic map, paleontological locality map) are easily compiled by choosing the associated data layers or by choosing the desired map under Bookmarks.

Figure 1. Shaded relief map of the onshore part of the Cambria 30´ x 60´ quadrangle, annotated with geographic names used in the text. Also shown is the 2003 M6.6 San Simeon earthquake epicenter. The main faults are shown as black lines.

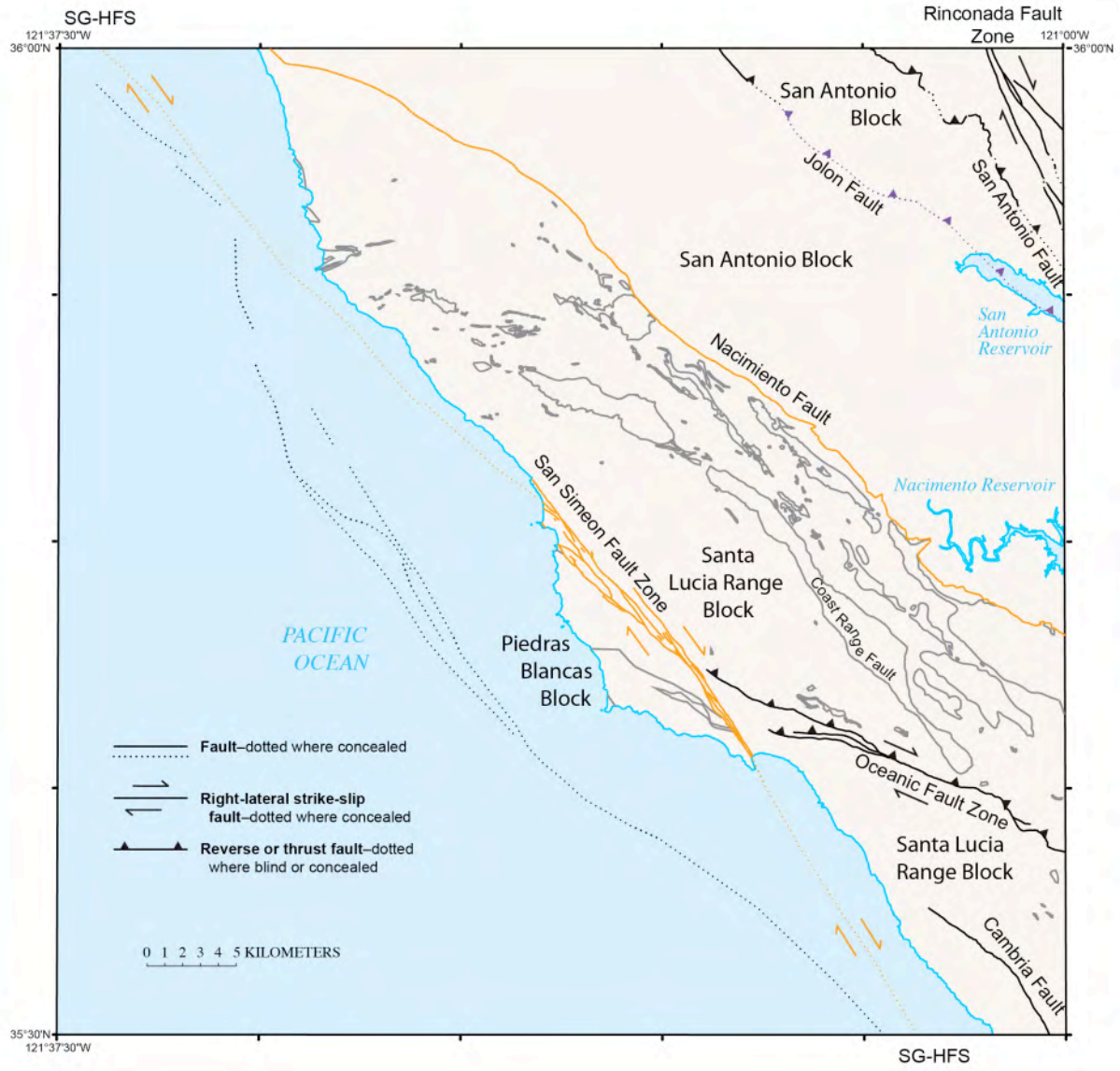

Figure 2. Index map of structural blocks and named faults in the map area. The complex Coast Ranges Fault is represented by gray lines. The newly mapped blind-fault reach of the Jolon Fault is shown as purple. Block-bounding faults are shown as orange. Faults of the San Gregorio-Hosgri Fault System are labeled SG-HFS. Also shown are traces of some offshore faults derived from bathymetric geomorphology as depicted on the U.S. Geological Survey topographic quadrangle. Reverse and thrust faults are shown with teeth on the hanging-wall side; right-lateral faults are shown by arrow pairs.

Stratigraphy

The stratigraphy[1] of the California Coast Ranges consists of three amalgamated Mesozoic and Paleogene basement complexes (Franciscan, Great Valley, Salinian) overlain by Tertiary and early Quaternary strata and Quaternary surficial deposits (fig. 3). Tertiary and early Quaternary strata differ across the map area, reflecting large-scale Tertiary and Quaternary offset on major faults as well as topographic separation of depositional basins, which necessitates subdivision of the Tertiary and Quaternary stratigraphy into three assemblages limited to major structural blocks (Piedras Blancas, Santa Lucia Range, San Antonio, see fig. 2).

Basement Complexes

Paleocene and Mesozoic rocks in the map area can be divided into three very distinctive rock suites that reflect the complex history of rock formation and accretion at the subduction margin of western North America throughout the Cretaceous and early Tertiary. Each basement complex represents a different part of the arc-forearc-accretionary prism subduction-margin system.

Salinian Complex

The Salinian complex is made up of Late Cretaceous plutonic rocks and older metamorphic wallrock, locally overlain unconformably by latest Cretaceous marine sedimentary rocks. Plutonic and metamorphic rocks represent magma chambers that underlay the Late Cretaceous continental-margin arc, as well as their host rocks. North of the map area, these rocks overlie Late Cretaceous pelitic schist along a folded thrust fault (fig. 4*A*; Ducea and others, 2009). The original position of the arc is known to have been south of the Sierra Nevada, because restoration of Tertiary San Andreas Fault slip places a distinctive gabbroic body (Logan Gabbro), now present in the southern San Francisco Bay region, with a correlative gabbroic body in the San Emigdio Mountains (fig. 4*B*). However, beyond that constraint, the original position is not known. Various workers have proposed competing hypotheses (for example Dickinson, 1983; Hall, 1991), but multiple lines of evidence strongly suggest that Salinia is equivalent to the San Emigdio, Mojave, and eastern Transverse Ranges blocks east of the San Andreas Fault (as summarized by Powell, 1993; fig. 4*B*).

[1] The U.S. Geological Survey standard for geologic maps is to use chronostratigraphic nomenclature (for example, lower Quaternary, Upper Cretaceous). However, in the California Coast Ranges, including the map area, deposition during periods of tectonic uplift, as well as tectonic juxtaposition of different stratigraphic sequences and interleaved terranes, has in many places resulted in older units being above younger units, even without overturning or structural repetition. As a result, we find the use of chronostratigraphic terms to be potentially confusing (such as middle Pleistocene marine terrace deposits everywhere above Upper Pleistocene marine terrace deposits) and instead use geochronologic nomenclature (for example, early Quaternary, Late Cretaceous), which is unambiguous, throughout.

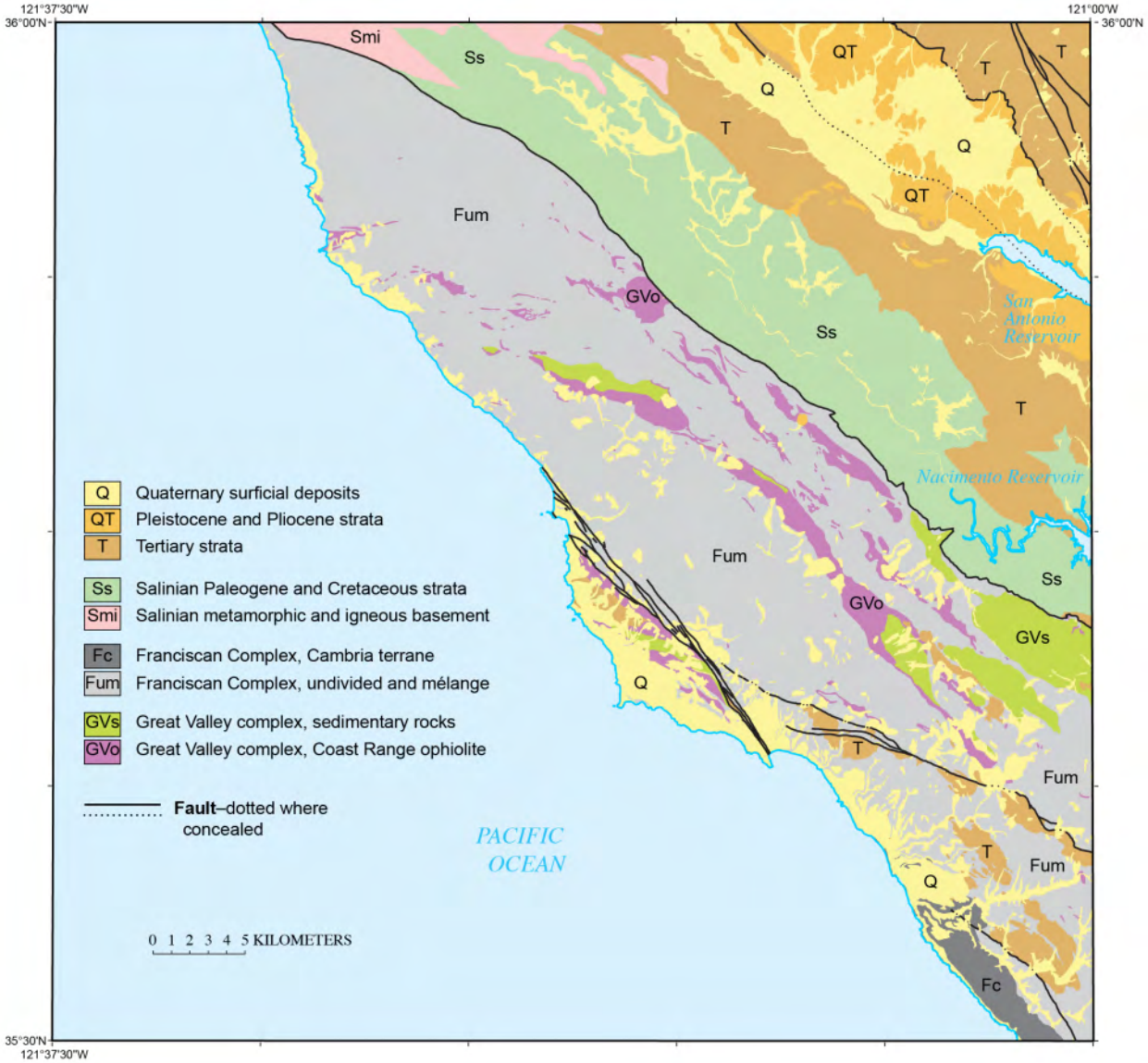

Figure 3. Index map of tectonostratigraphic elements in the map area, showing the distribution of Quaternary surficial deposits, Pleistocene and Tertiary strata, and early Tertiary and Mesozoic basement complexes. See figure 2 for structural block and fault labels.

A

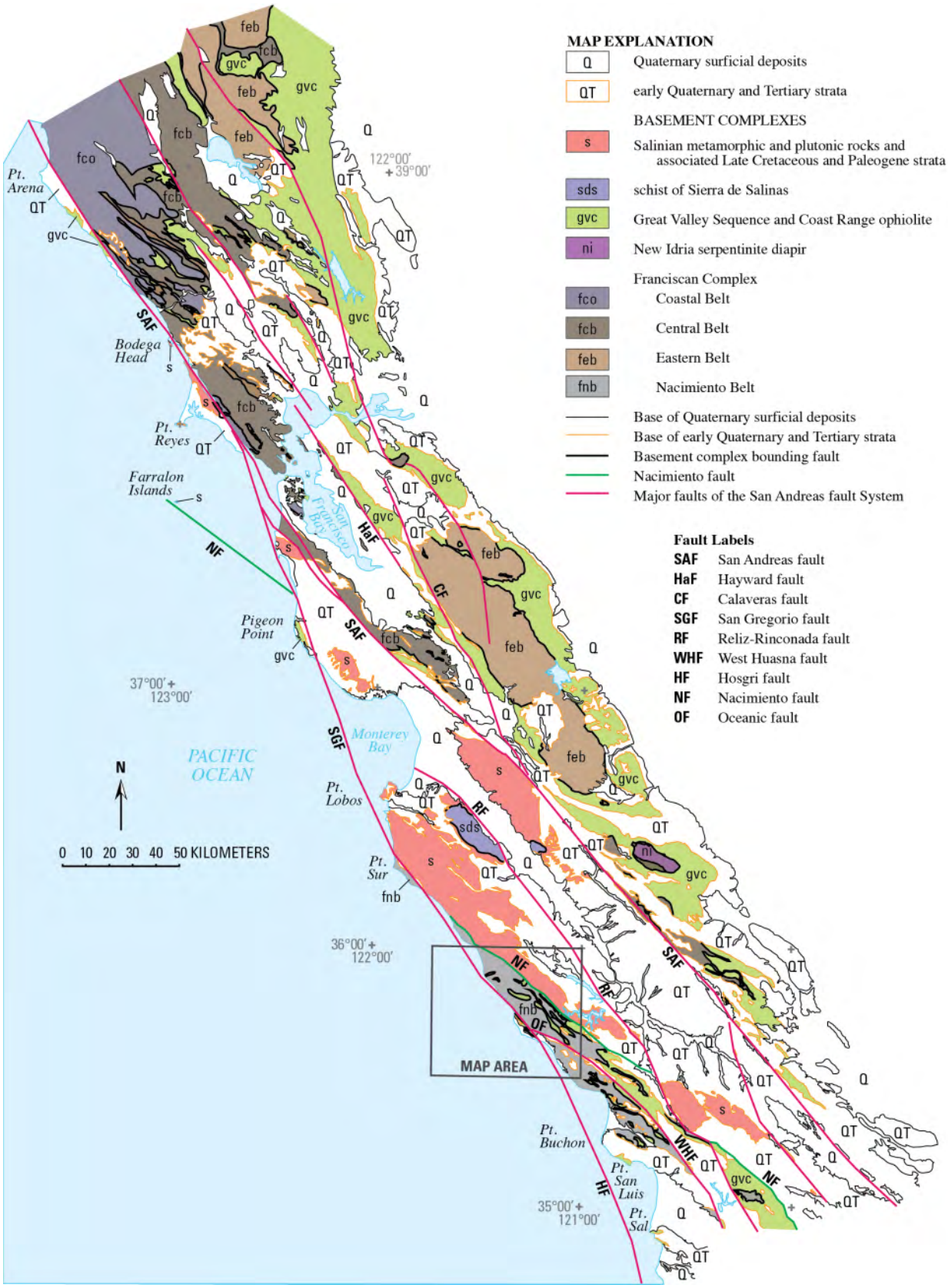

Figure 4–See caption, p. 10

B

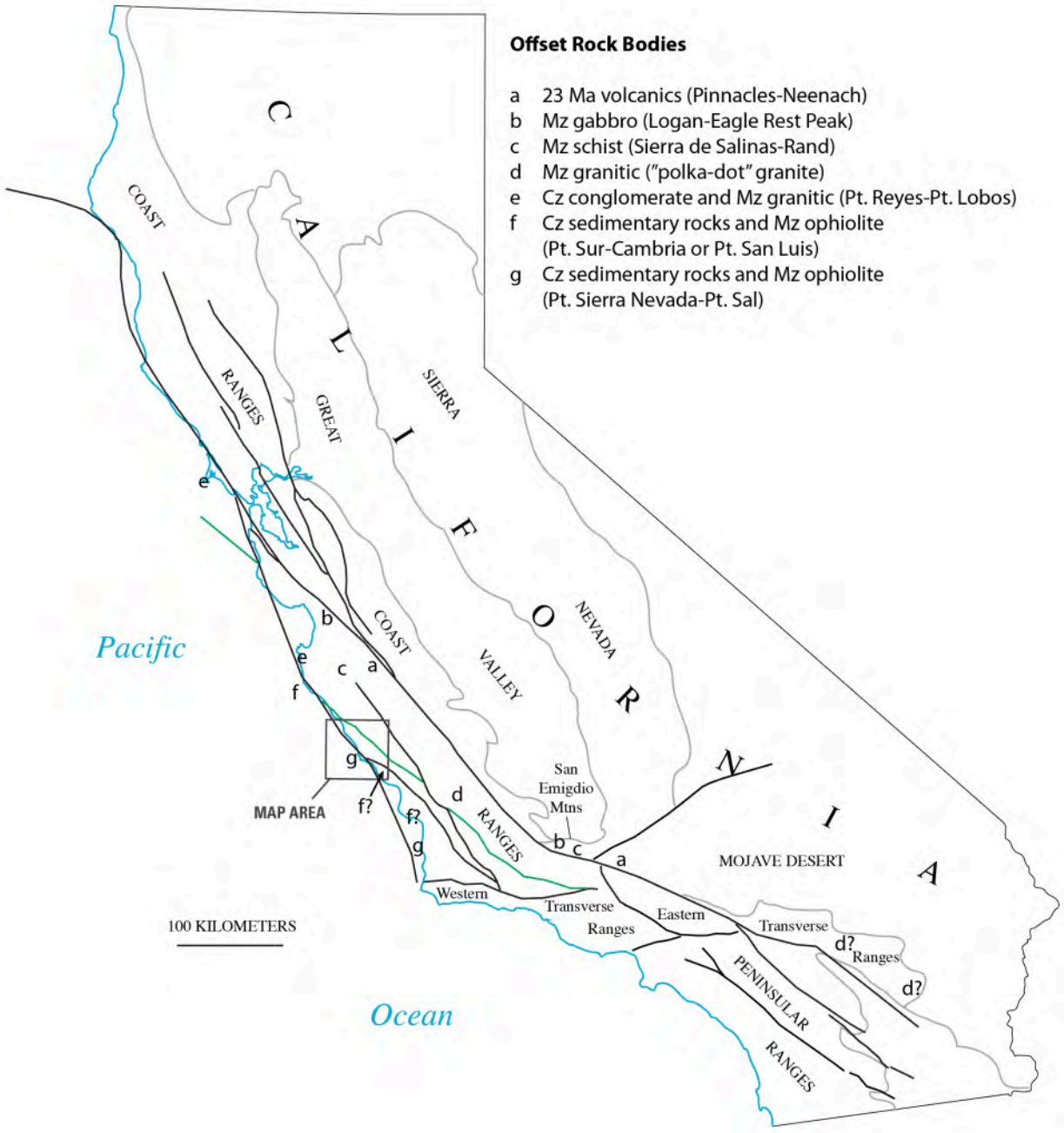

Figure 4–See caption, p. 10

C

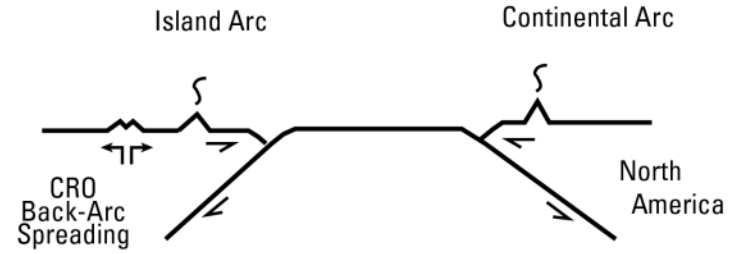

Accreted ophiolite formed in the back-arc of an east-facing ocean-island arc

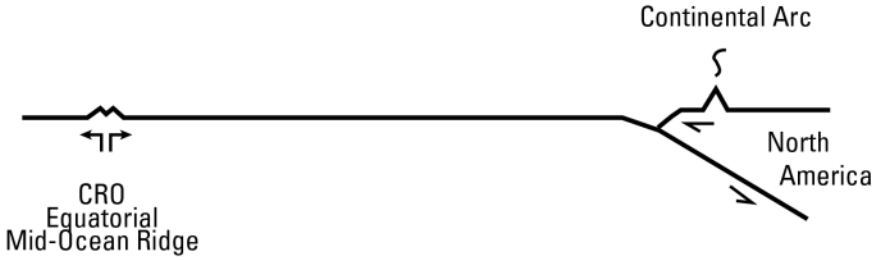

Far-travelled mid-ocean ridge ophiolite

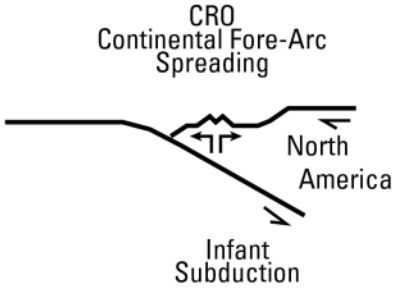

Autochthonous ophiolite formed in the continental-margin forearc

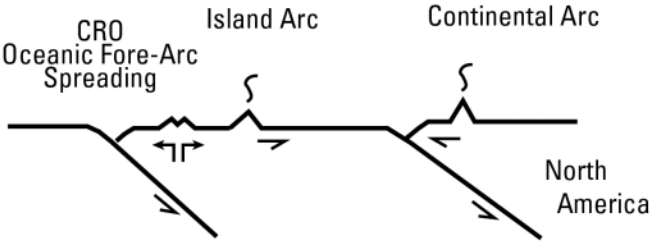

Rifting in the forearc basin of an island arc that then accreted

Figure 4–See caption, p. 10

Figure 4. Maps and cross sections illustrating the tectonostratigraphic setting and history of the study area. *A.* Overview map of tectonostratigraphic elements in the northern and central California Coast Ranges; *B.* Index map of California showing the main strands of the San Andreas Fault System (black) and the Nacimiento Fault (green), along with a number of geographic provinces, mountain ranges, and rock bodies offset by fault slip mentioned in the text; *C.* Cartoon tectonostratigraphic cross sections illustrating various models of Coast Range ophiolite (CRO) formation (Dickinson and others, 1996; Blake and others, 2002).

What is clear, however, is that the Salinian arc basement was rapidly unroofed in latest Cretaceous time, bringing the plutonic and metamorphic rocks now in the map area to the surface as the depositional base for a thick sequence of Maastrichtian (latest Cretaceous) marine strata (in the map area, made up of the El Piojo, Shut-in, Italian Flat, and Steve Creek Formations). This depositional environment continued at least into the Paleocene (as shown in the map area by the overlying Piedras Altas Formation).

Great Valley Complex

The Great Valley complex in the Cambria quadrangle is composed of three parts: the basal Jurassic Coast Range ophiolite, unconformably overlain by Late Jurassic and Early Cretaceous Toro Formation, in turn unconformably overlain by the Cretaceous Atascadero Formation. The basal ophiolite in the Cambria area has been included in the Coast Range ophiolite, which also makes up the base of the Great Valley complex present east of the San Andreas Fault (fig. 4*A*). However, restoration of Neogene offset on the San Andreas Fault places the Coast Range ophiolite in the map area 300 km or more southeast of the correlated ophiolite east of the San Andreas Fault. The Cambria region ophiolite may also have been affected by large-scale offset related to transport of the Salinian Complex. Therefore the Coast Range ophiolite in the map area may not be genetically related to the Coast Range ophiolite to the east. Nevertheless, we summarize four genetic models for the Coast Range ophiolite here, even though much of the underpinning of these models is based on observations of the unit east of the San Andreas Fault. We note that the ophiolite bodies in the two regions are the same age and same geochemical composition, so the genetic setting of the two may be similar. Furthermore, some of the data incorporated into the genetic models does come from the ophiolite in or near the map area. At the very least, the models outlined below are plausible models for the ophiolite in the map area.

The Coast Range ophiolite formed between about 173 and 164 Ma (Blake and others, 1992; Hagstrum, 1997; Hopson and others, 1997), but the tectonic setting of ophiolite formation is controversial. Dickinson and others (1996) summarize three different models: accreted ophiolite formed in the back-arc of an east-facing ocean-island arc, far-travelled mid-ocean ridge ophiolite, and autochthonous ophiolite formed in the continental-margin forearc (fig. 4*C*). More recently, Graymer and his coauthors in Blake and others (2002) proposed a fourth model that took into account additional data, including the nature of coeval rocks in the Sierra Nevada that reflect the tectonic setting of ophiolite formation, as well as the age of the oldest Franciscan Complex metamorphism. In that model, the ophiolite formed by rifting in the forearc basin of an island arc that then accreted to the North American margin in Late Jurassic (Kimmeridgian, ~153 Ma) time (fig. 4*C*; see Graymer, 2005, for details of the timing of accretion).

The ophiolite is unconformably overlain by late Jurassic and Cretaceous marine sedimentary rocks of the Great Valley sequence, represented in the map area by the Toro Formation and overlying Atascadero Formation. In the central California Great Valley, these

strata formed in the forearc of the North American continental margin volcanic arc (Dickinson, 1971; Hamilton, 1978) after accretion of the Jurassic island arc and Coast Range ophiolite (Blake and others, 2002; Graymer, 2005). The Toro and Atascadero Formations were deposited far south of the present-day Great Valley, but lithologic and petrologic similarity between the Great Valley sequence to the north and in the map area argues for a similar depositional environment.

Franciscan Complex

The rocks of the Franciscan Complex are mostly derived from Jurassic to Cretaceous oceanic crust and pelagic deposits overlain by Upper Jurassic to lower Tertiary turbidites. These rocks were variably metamorphosed, depending on the depth of subduction prior to unroofing, from high-grade glaucophane schist to incipient prehnite-pumpellyite facies. In the northern Coast Ranges (fig. 4*A*), the Franciscan Complex is made up of three structural belts: an Eastern Belt composed of Jurassic and Cretaceous coherent medium- to low-grade blueschist metamorphic rocks (lawsonite-albite and lawsonite-jadeite-quartz sub-facies); a Central Belt composed of slabs of coherent Jurassic and Cretaceous low-grade metavolcanics and metasediments (prehnite-pumpellyite facies) interleaved within mélange; and a Coastal Belt composed mostly of Late Cretaceous and Tertiary, low-grade metasediments (laumontite facies). The position of these belts reflects the order of accretion and depth of subducition of Franciscan Complex terranes. The earliest-accreted Eastern Belt rocks are also farthest subducted and most metamorphosed, whereas the last-accreted Coastal Belt rocks are least subducted and metamorphosed. The belts are further divided into tectonostratigraphic terranes, large fault-bounded blocks with an internally consistent stratigraphy and metamorphic grade (for example, Blake and others, 1982). Mélange is not considered part of any terrane, but rather a tectonic mixture of rocks from multiple terranes (Blake and others, 2002).

Franciscan Complex rocks in the Cambria region are part of the Nacimiento Belt (fig. 4*A*). They can be roughly subdivided into three main lithologic categories: (1) coherent and nearly coherent bodies that retain recognizable sedimentary layers and contain Cretaceous microfossils (Hsu, 1969; Smith, 1978; Seiders, 1989a); (2) broken formation in which original bedding is entirely or almost entirely disrupted, but rock types are largely unmixed and exotic blocks (serpentinite, high-grade metamorphic blocks) are missing; and (3) mélange composed of sheared sedimentary matrix containing blocks of sandstone and metasandstone, chert and metachert, basalt and greenstone, serpentinite, and blueschist. This suite of rock types most resembles the Central Belt; rocks like those of the other belts are not found in the map area. The similarity of lithology, as well as age, suggests that Franciscan Complex rocks of the Nacimiento Belt are correlative with the Central Belt. The relatively coherent Late Cretaceous metasedimentary rocks near Cambria can be assigned to a terrane, herein called the Cambria terrane. As mentioned above, mélange is not considered part of any terrane, and in the map area the broken formation presently lacks the needed lithologic and stratigraphic data to determine whether it should be considered part of the Cambria terrane or some other terrane(s).

A model for the tectonic history of all Franciscan Complex terranes follows: oceanic rocks (including mid-ocean-ridge basalts and seamounts); overlain by pelagic and detrital sediments; brought into proximity with North America by convergent plate motion; and more or less subducted, accreted, and moved northward to their current position on the continent by transform offset along the continental margin. Earlier workers (Howell and others, 1977) have

suggested that the Cambria terrane was deposited as a trench basin, formed within the accretionary prism and subsequently structurally interleaved with older accreted rocks.

Early Quaternary and Tertiary Strata

Early Quaternary and Tertiary strata in the Cambria region are divided into three distinct assemblages bounded by major faults (fig. 2): the Piedras Blancas block, the Santa Lucia Range block, and the San Antonio block. These assemblages represent geographically distinct depocenters of strata, juxtaposed by large-scale offset on their bounding faults. Topographic separation of the Santa Lucia Range and San Antonio blocks in Pliocene and younger time has also resulted in deposition of different rock types.

Piedras Blancas Block

The Piedras Blancas block lies west of the San Simeon Fault along the coast in the west-central part of the onshore map area. Amalgamated Franciscan Complex and Great Valley complex basements are overlain unconformably by early Miocene to Pliocene strata. These rocks probably reflect a depocenter once located relatively about 90 km south of their present location, brought to their present position relative to rocks farther east by right-lateral offset on the Hosgri-San Simeon Fault (Hall, 1975; Jachens and others, 2009; Langenheim and others, 2013).

Santa Lucia Range Block

The Santa Lucia Range block lies between the San Simeon and Nacimiento Faults. Like the Piedras Blancas block it is composed of amalgamated Franciscan Complex and Great Valley complex basements, here overlain unconformably by Oligocene to Pliocene strata. The Tertiary strata differ from the Piedras Blancas strata in the presence of Oligocene and Miocene volcanic units, along with other differences discussed below in the Description of Map Units. The bulk of the Tertiary rocks in this block crop out south of the Oceanic Fault, probably due to relatively greater erosion in the more uplifted northern hanging wall of this reverse fault.

San Antonio Block

The San Antonio block lies between the Nacimiento and Rinconada Faults. Unlike the other blocks, the basement of this block is composed of Salinian complex rocks. Also unlike the other blocks, there is not a universal unconformity between Mesozoic and Cenozoic units, but in places a continuous latest Cretaceous to Paleocene stratigraphy is preserved. Instead, there is a block-wide unconformity between late Oligocene and early Miocene strata and underlying Paleogene strata. Oligocene and Miocene strata in this block have been given the same names as roughly coeval strata in the Santa Lucia Range block, but, as described below, the rock types and depositional environments of the units in the two blocks are distinct, so presumption of original continuity or proximity is ill advised.

Quaternary Surficial Deposits

Quaternary surficial deposits in the map area are mostly undivided. The exceptions are beach sand and marine terraces along the Pacific coast, river terraces along the San Antonio River and other major drainages, and older alluvial fan deposits in Lockwood Valley

A series of discrete marine terrace surfaces were adapted from a Quaternary map of the San Simeon region produced by Weber (1983). The locations of a few of these surfaces in the vicinity of San Simeon Point were later revised by Hanson and others (1994). Both sources originated as paper maps, which were scanned, georeferenced, and later digitized in ArcGIS. To better fit the 1:100,000 scale, some of the smallest terrace remnants were not included, and other contacts were modified as needed. The names and age designations of marine terraces are based on each surface's relative elevation above mean sea level and degree of erosional modification. Correlation of these terraces is derived from the estimated local tectonic uplift rates as discussed by Weber (1983).

Paleontology

Many different kinds of fossils have proved invaluable to understanding the geology of the map area: microfossils, including radiolaria, foraminifers, and pollen in the Franciscan Complex; mollusks in the Great Valley and Salinian complex sedimentary rocks as well as the overlying Tertiary strata; and foraminifers and diatoms in the Monterey Formation. A complete listing of the fossils in the map area is beyond the scope of this report, but we make extensive reference to fossil data in the discussions below.

A majority of the microfossil data used in this study are derived from samples in the U. S. Geological Survey collections currently housed in the Micropaleontology Laboratory in Flagstaff, Arizona, and Chevron Oil Company slides borrowed from the California Academy of Sciences in San Francisco, California, and reported in Malmblorg and others (2008). Assemblages were reviewed for consistency with modern biostratigraphic understanding and revisions were made as appropriate. Age interpretations use the correlation of the benthic foraminiferal stages and zones to the international time scale as discussed in McDougall (2008). Cenozoic environmental interpretations are based on an overview of California benthic foraminifers by Ingle (1980), Ingle and Keller (1980), and Blake (1981, 1991) and studies of cosmopolitan benthic foraminifers by Douglas (1981) and van Morkhoven and others (1986). We have intentionally not used all of the foraminiferal data in the published record for the map area in the discussion that follows. The data we chose not to use falls into one of three categories:

1. Locality descriptions of some samples that were inadequate and that could not be located with any certainty or that plotted on the "wrong" side of a contact. We interpret this to indicate that either the locality or the contact are slightly misplaced, but it is beyond the scope of this study to try to reoccupy the localities to determine whether the locality or contact need to be relocated.
2. Data that seems "obviously wrong" (for example, a late Miocene locality in a unit overlain by well-documented middle Miocene strata). We leave the detailed mapping of the structures required to explain such data, if in fact they are correct, to future workers.

3. Less restrictive fossil ages in a unit that has an age more constrained by other stratigraphic data. For example, some units in the Salinian Cretaceous may include only Late Cretaceous foraminifers, but the unroofing history of Salinian basement, as well as more robust foraminiferal data from adjacent areas, limit all Salinian Cretaceous strata in the map area to Maastrichtian or younger.

Microfossil samples were examined from all three structural blocks. Although faunas are sparse in the Piedras Blancas and Santa Lucia Range blocks, foraminiferal faunas in the San Antonio block are common. The samples examined are listed in the paleontological data files (CambriaPaleoLocality.xlsx) along with the age and ecological interpretations. Faunal lists are given for selected samples (CambriaPaleoChecklist.xlsx). In general, these assemblages indicate that the Vaqueros Formation was deposited at upper bathyal depths (150–500 m), and deposition of the Monterey Formation began in the upper middle bathyal depths (500–1,500 m) then shallowed to upper bathyal depths (150–500 m).

Radiometric Ages

Four units in the map area have been analyzed using radiometric dating techniques. Ernst and others (2011) report U-Pb zircon ages of 26.8±0.3 and 27.4±0.4 Ma for two samples of the Cambria Felsite (Tc). Zircons from the Coast Range ophiolite in the Piedras Blancas block (Mattinson and Hopson, 2008) yielded a U-Pb age of 165.580±0.038 Ma. Detrital zircon analysis has yielded a maximum depositional age of ~17 Ma for the Lospe Formation in the Piedras Blancas block (J. Colgan, written commun., 2011), 77–90 Ma (Morisani and others, 2005) for some slabs of Franciscan Complex graywacke in mélange in the Santa Lucia Range block, and about 80–90 Ma (Jacobson and others, 2011) for Franciscan Complex graywacke from the Cambria terrane.

Geophysical Data

Gravity and magnetic data are useful for projecting the surface geology into the subsurface. Gravity data are processed to reflect density variations within the upper and middle crust and are particularly well suited for determining the shape of Cenozoic basins, because of the significant density contrast between dense Mesozoic basement rocks and lighter Cenozoic rocks. Magnetic data reflect magnetization variations within the crust and are well suited for mapping the distribution of rock types that contain magnetite. Both gravity and magnetic anomalies can be related to rock type, providing a means to map remotely some aspects of the geology.

About 671 onshore gravity measurements were used to produce an isostatic gravity map of the quadrangle (fig. 5). Offshore, the gravity data are from a 6-km grid (Decade of North American Geology Project, 1987). Sources of data include the agency formerly known as Defense Mapping Agency, Burch and others (1971), and Pan-American Center for Earth and Environmental Studies (2010). Gravity measurements are non-uniformly distributed in the region, with an average spacing of 1 km.

Gravity data were reduced to free-air anomalies using standard formulas (for example, Telford and others, 1976). Bouguer, curvature, and terrain adjustments to a radial distance of 166.7 km were applied to the free-air anomaly at each station to determine the complete Bouguer

A

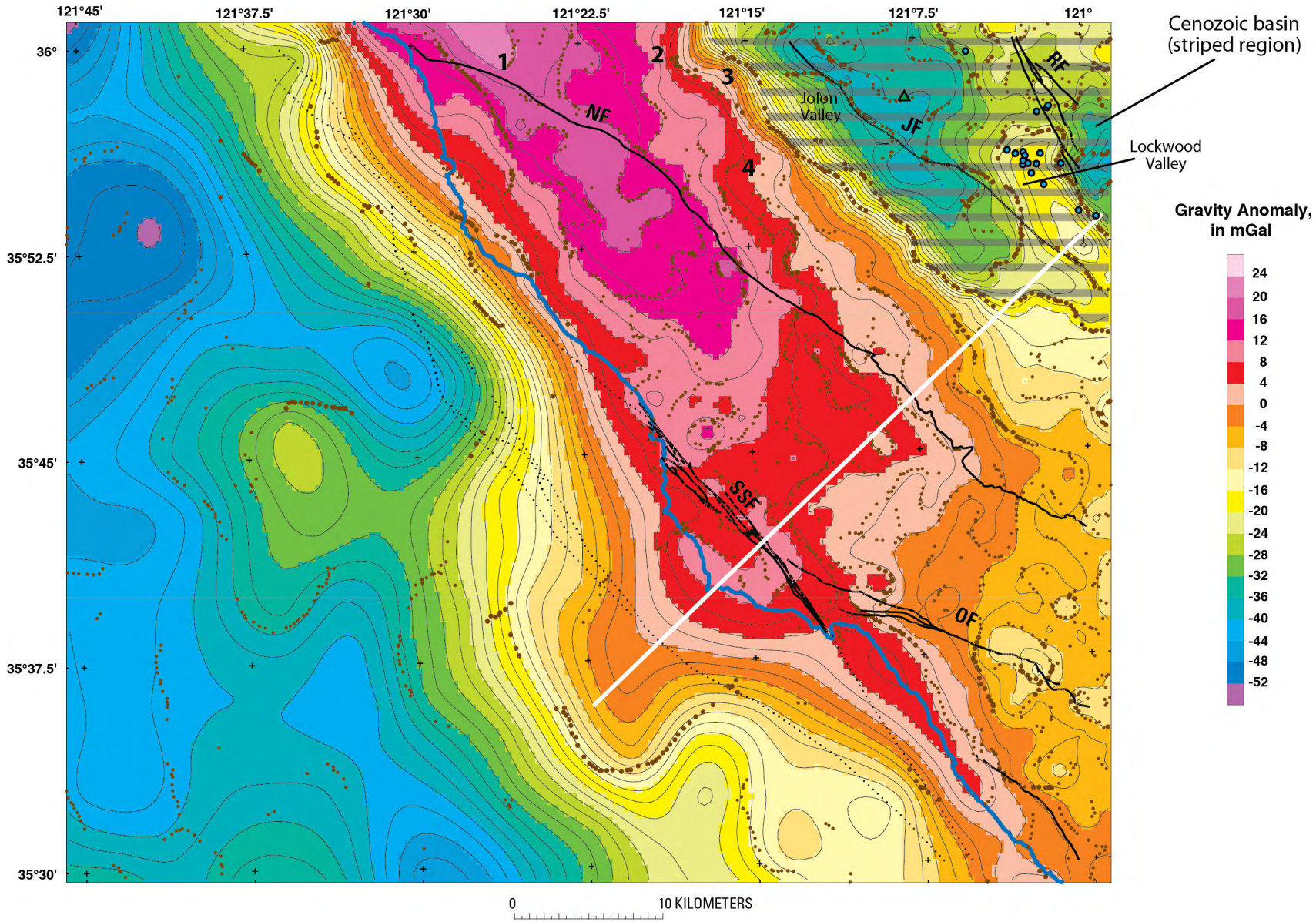

Figure 5–See caption, p. 17

B

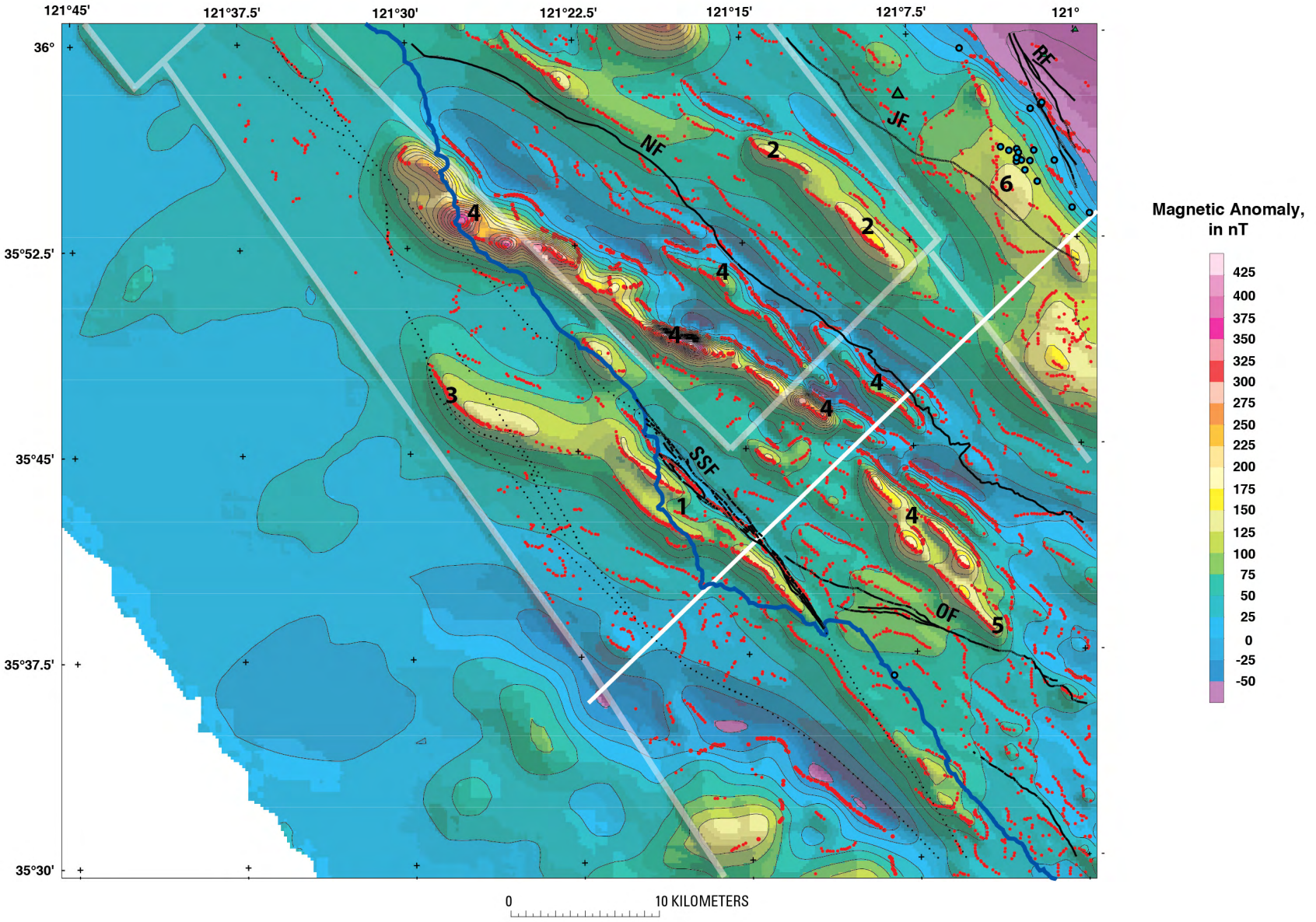

Figure 5–See caption, p. 17

Figure 5. *A.* Color isostatic gravity map of the eastern three-quarters of the Cambria 1:100,000-scale quadrangle. Light black lines, 2 mGal contours. Dotted and heavy black lines, faults. Brown dots, locations of density boundaries from maximum horizontal gravity gradient. White line, location of cross section shown in fig. 6. JF, Jolon Fault; NF, Nacimiento Fault; OF, Oceanic Fault; RF, Rinconada Fault; SSF, San Simeon Fault. Black-rimmed blue dots are drillholes that penetrated basement rocks at shallow depth. The green triangle is a drillhole that bottomed in Miocene sedimentary rocks at nearly 1.8 km depth. 1, gravity high attributed to metamorphic rocks of the Salinian complex; 2, easternmost extent of continuous exposure of Salinian complex rocks; 3, isolated outcrop of Salinian basement; 4, outcrops of latest Cretaceous sedimentary rocks. *B.* Color shaded-relief aeromagnetic map of the eastern three-quarters of the Cambria 1:100,000-scale quadrangle. Thin black lines, 25 nT contours. Pale-gray lines, aeromagnetic survey boundaries. Dotted and heavy black lines, faults. Red dots, locations of magnetization boundaries from maximum horizontal gradient. JF, Jolon Fault; NF, Nacimiento Fault; OF, Oceanic Fault; RF, Rinconada Fault; SSF, San Simeon Fault. Black-rimmed blue dots are drillholes that penetrated basement rocks at relatively shallow depth. The green triangle is a drillhole that bottomed in Miocene sedimentary rocks at nearly 1.8 km depth. 1, outcrop of Lospe Formation; 2 and 6, magnetic highs attributed to concealed Salinian basement rocks; 3, northwest edge of magnetic rocks interpreted to be truncated by offshore faults; 4, magnetic highs coincident with outcrops of diabase and serpentinite; 5, truncation of magnetic rocks interpreted to be truncated by Oceanic Fault.

anomalies at a standard reduction density of 2,670 kg/m^3 (Plouff, 1977). An isostatic adjustment was then applied to remove the long-wavelength effect of deep crustal and (or) upper mantle masses that isostatically support regional topography. The isostatic adjustment assumes an Airy-Heiskanen model (Heiskanen and Vening-Meinesz, 1958) of isostatic compensation. Compensation is achieved by varying the depth of the model crust-mantle interface, using the following parameters: a sea-level crustal thickness of 25 km, a crust-mantle density contrast of 400 kg/m^3, and a crustal density of 2,670 kg/m^3 for the topographic load. These parameters were used because (1) they produce a model crustal geometry that agrees with seismically determined values of crustal thickness for central California, (2) they are consistent with model parameters used for isostatic corrections computed for the rest of California (Roberts and others, 1990), and (3) changing the model parameters does not significantly affect the resulting isostatic anomaly (Jachens and Griscom, 1985). The resulting isostatic residual gravity values should reflect lateral variations of density within the middle to upper crust. Accuracy of the data is estimated to be on the order of 0.1 to 0.5 mGal.

The aeromagnetic map is based on data from four surveys of varying resolution (table 1). The onshore surveys (U.S. Geological Survey, 2005; Langenheim and others, 2009) were flown at a nominal height of 245–305 m (800–1,000 ft) above ground along flight lines spaced 0.54 to 0.8 km (0.33 to 0.5 mi) apart. Accuracy of these modern surveys is 1 nanotesla or better. The offshore survey ((McCulloch and Chapman, 1977) was flown at a constant barometric altitude of 610 m along flight lines 1.6 km apart. All data were adjusted to a common magnetic datum and then merged by smooth interpolation across a buffer zone along the survey boundaries.

To help delineate structural trends and gradients expressed in the gravity and magnetic fields, a computer algorithm was used to locate the maximum horizontal gradient (Cordell and Grauch, 1985; Blakely and Simpson, 1986). Concealed basin faults beneath the valley areas were mapped using horizontal gradients in the gravity field. We calculated magnetization boundaries on a filtered version of the magnetic field to enhance shallow sources. First, we subtracted a numerically derived regional field from the actual merged data. The regional field was computed by analytically continuing the merged aeromagnetic data to a surface 200 m higher than that on which the measurements were made, an operation that tends to smooth the data by attenuating short-wavelength anomalies (Blakely, 1995). Second, the resulting residual aeromagnetic field was mathematically transformed into magnetic potential anomalies (Baranov, 1957); this procedure effectively converts the magnetic field to the

equivalent gravity field that would be produced if all magnetic material were replaced by proportionately dense material. The horizontal gradient of the magnetic potential field was then calculated. Gradient maxima occur approximately over steeply dipping contacts that separate rocks of contrasting densities or magnetizations. For moderate to steep dips (45° to vertical), the horizontal displacement of a gradient maximum from the top edge of an offset horizontal layer is always less than or equal to the depth to the top of the source (Grauch and Cordell, 1987).

Table 1. Specifications of aeromagnetic surveys within the Cambria quadrangle.

Survey	Year flown	Altitude	Flightline spacing (km)	Flightline direction
Paso Robles (Langenheim and others, 2009)	2008	305 m above ground	0.8	NE./SW.
Salinas Valley South (U.S. Geological Survey, 2005)	2002	244 m above ground	0.54	NE./SW.
Carmel (this report)	2009	305 m above ground	0.8	NE./SW.
California Coast (McCulloch and Chapman, 1977)	1976	610 m barometric	1.6	NE./SW.

Gravity Anomalies

Gravity anomalies within the Cambria quadrangle (fig. 5*A*; Gravity Map, see PDF) reflect the density contrast between dense Mesozoic basement rocks and overlying, less dense Cenozoic sedimentary rocks and deposits. The lowest gravity values on land are located in the northeast corner of the map where Miocene and younger rocks are exposed in Jolon, Lockwood, and San Antonio Valleys. The highest gravity values correspond to outcrops of metamorphic rocks of the Salinian complex in the north-central part of the map (1 in fig. 5*A*). These rocks, the southern tip of an elongate northeast-tilted section of the Coast Ridge Belt that mostly crop out north of the quadrangle, likely represent exposures of the deepest and more mafic parts of the continental margin arc, with calculated seismic velocities of approximately 6.5 km/s (Ducea and others, 2003). The eastward decrease in gravity values measured on these metamorphic and plutonic rocks along the north-central edge of the quadrangle (region between 1 and 2 in fig. 5*A*) may reflect, in part, the transition from dense, lower crustal rocks to more felsic, mid-crustal rocks within the Salinian complex. An outcrop of Salinian basement surrounded by Miocene sedimentary rocks (3 in fig. 5*A*) contains an even tighter, 6-mGal gradient, which is likely caused by faults associated with the edge of a Cenozoic basin (striped region in fig. 5*A*). Gravity values also gradually decrease southeastward from Salinian basement complex outcrops to outcrops of latest Cretaceous sedimentary rocks (such as units Ksc, Kep, and Ku on Gravity Map (see PDF); 4 in fig. 5*A*) that overlie the basement complex.

Gravity values also decrease very gradually to the south-southeast from the highest values on Salinian complex basement onto outcrops of Franciscan Complex across the Nacimiento Fault. The source of the gravity high across the fault was attributed tentatively by Burch and others (1971) to topography composed of rocks with a density of 2,800 kg/m^3; however, the gravity high persists if the data are reduced to a density of 2,800 kg/m^3. The source of the higher values is not known but could be deeply buried, given the broad, nearly 20-km width of the southeast gradient of the high. The

Nacimiento Fault does not coincide with a prominent gravity gradient but rather a slight, northwest-trending gradient, where slightly denser Franciscan Complex is juxtaposed against less dense latest Cretaceous Salinian strata. Given that the Nacimiento Fault marks a significant seismic-velocity contrast but no significant gravity gradient to the southeast of the Cambria quadrangle (Howie and others, 1993), the absence of a strong gravity gradient coupled with a prominent seismic velocity contrast suggests that the fault places relatively coherent, higher-velocity Salinian complex rocks (granite and gneiss) against fractured, lower-velocity Franciscan Complex rocks (as exemplified by units of mélange and broken formation). Fractures can reduce seismic velocity significantly without a corresponding reduction in density (Stierman and Kovach, 1979). No active-source seismic refraction data are available for the Cambria quadrangle. A statewide California tomographic model (Lin and others, 2010) does not show much of a velocity contrast across the Nacimiento Fault in this area, but that likely reflects the low resolution (10–20 km grid spacing) and smoothing of the model.

The most prominent and steepest gravity gradient marks the southwest edge of a Cenozoic basin beneath Jolon and San Antonio Valleys in the northeast part of the quadrangle. The amplitude of the gravity low within the quadrangle is about 40–50 mGal; using an infinite slab approximation and assuming an average density contrast of 400 kg/m^3, Mesozoic basement is 2.4 km to 3.0 deep. This is consistent with an oil-test drill hole (triangle in fig. 5*A*) that bottomed in Miocene rocks at a depth of 1.8 km close to the lowest gravity values in the basin (California Division of Oil, Gas, and Geothermal Resources, 1982) and with a cross section by Graham and others (1991) based on drill-hole data along the northern margin of the quadrangle. However, gravity values are not uniformly low in Jolon Valley. Gravity values in Lockwood Valley are as much as 20 mGal higher than the lowest values in the basin and the relative gravity high coincides with several oil test drill holes that intercepted granitic basement at depths between 150 m and 730 m (black-rimmed blue circles in fig. 5*A*). We interpret this shallow granite as uplifted in the hanging wall of the Jolon Fault, discussed in more detail below. The eastern edge of the basement high is bounded by the Rinconada Fault.

Magnetic Anomalies

Sources of magnetic anomalies are those rock types that contain magnetite. In the central Coast Ranges, these rock types are serpentinite, gabbro, and diabase of the Coast Ranges ophiolite, some basement rock types within the Salinian complex (such as granodiorite exposed in the La Panza Range southeast of the Cambria quadrangle), metavolcanic rocks of the Franciscan Complex, and locally Miocene mafic volcanic rocks. In general, sedimentary rocks do not produce pronounced aeromagnetic anomalies, but lower-amplitude magnetic highs may be associated with sedimentary strata that are rich in mafic/ultramafic clasts or magnetite grains. In the map area, the Lospe Formation in the Piedras Blancas block is locally magnetic because of ophiolitic clasts but is too thin to produce a significant anomaly. Where it crops out, it coincides with a local magnetic low relative to the ophiolite (1 in fig. 5*B*). Mafic clasts in conglomerate may be the cause of two low-amplitude magnetic highs (2 in fig. 5*B*) in the Salinian Cretaceous strata southwest of Jolon Valley; however, the broad wavelength of these anomalies suggests a source within the basement.

In the Piedras Blancas and Santa Lucia Range blocks, prominent, short-wavelength, curvilinear magnetic anomalies coincide well with outcrops of Coast Range ophiolite (Magnetic Map, see PDF). The San Simeon Fault clearly forms the eastern margin of the anomalies associated with ophiolite in the Piedras Blancas block. These anomalies become broader and more diffuse to the northwest, consistent with deeper magnetic basement offshore, but they cannot be traced west of the continental slope. The northwest edge of these anomalies (Magnetic Map, see PDF; 3 in fig. 5*B*) also coincides with a mapped offshore fault.

A band of short-wavelength magnetic anomalies (4 in fig. 5*B*) trend northwest to west-northwest across the Santa Lucia Range block and coincide with discontinuous outcrops of Jurassic diabase and serpentinite (Magnetic Map, see PDF). Note that the cross section (white line in fig. 5*B*) crosses this band of anomalies where the anomaly amplitudes are somewhat muted, indicating that the geometry of mafic bodies shown on the cross section (fig. 6) may be thicker and more deeply penetrating out of the plane of the section. Southwest of the magnetic anomalies, the magnetic field is relatively smooth, interrupted by a few small anomalies associated with scraps of serpentinite and an outcrop of Franciscan Complex metavolcanic rocks. Extensive outcrops of Franciscan Complex mélange, greywacke, and broken formation are characterized by a relatively smooth magnetic field.

The southwesternmost of the Santa Lucia Range magnetic-anomaly bands appears to terminate at its southeast end (5 in fig. 5*B*) just north of the Oceanic Fault, suggesting that the fault cuts off the source of the anomalies. Its northwest end is likely truncated by the offshore extension of the San Simeon Fault. Along its northeast margin, it coincides locally with the Nacimiento Fault.

The magnetic anomalies in the San Antonio block differ from those south of the Nacimiento Fault. They are broader and the sources of the anomalies are concealed beneath Cretaceous and younger cover. A magnetic anomaly in the northeast part of the quadrangle (6 in fig. 5*B*) coincides approximately with a gravity high, suggesting that the granitic basement is the source of the anomaly. Its northeast margin coincides with the Rinconada Fault and correlating these buried rocks with magnetic rocks exposed in the La Panza Range suggests a cumulative offset of about 38 km along the Rinconada Fault (Jachens and others, 2009). The offset estimate from the magnetic anomalies is supported by independent estimates based on geologic data of Graham (1978) and Grove (1993).

Structure

The map area is composed of three major structural blocks separated by two large-offset northwest-trending faults (figs. 2, 5*A*). Although broken up by other faults, including some seismogenic and Quaternary-active faults, the major structural blocks represent a relatively coherent tectonostratigraphic entity that includes the same basement and overlying stratigraphic sequence throughout, which differ from those of adjacent major structural blocks. The differences in composition of adjacent blocks suggest significant offset on the bounding faults needed to juxtapose rock bodies originally formed in distinct depositional environments. The Nacimiento Fault separates Salinian basement and overlying strata of the San Antonio block from the Franciscan Complex/Great Valley complex basement and overlying strata of the Santa Lucia Range block. The Hosgri-San Simeon Fault Zone is part of the San Andreas plate-margin fault system and separates the lithologically similar—but not identical—Piedras Blancas and Santa Lucia Range blocks. The Nacimiento Fault is a steeply northeast dipping structure (as shown by the dip of the surface trace and suggested by the aeromagnetic data, fig. 5*B*), whereas the San Simeon Fault is near vertical (as shown by elocated hypocenters, fig. 7, and aeromagnetic data, fig. 5*B*).

A

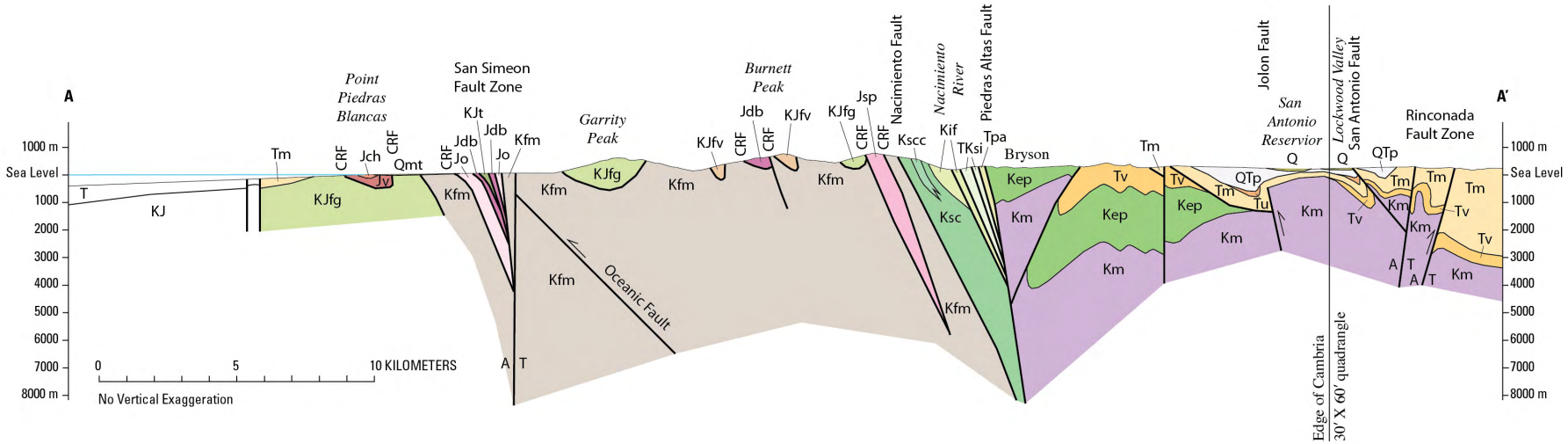

Figure 6. *A*. Cross section of the map area and an adjacent area to the east, through Point Piedras Blancas and San Antonio Reservoir. The adjacent area is added to show the Rinconada Fault Zone and San Antonio Fault which lie in the map area to the north of the cross-section line. Geology in the adjacent area is based on Durham (1974) and Graham and others (1991). CRF = Coast Ranges Fault. Undifferentiated units in the offshore subsurface are shown as T (Tertiary) and KJ (Cretaceous and (or) Jurassic); *B*. Gravity and magnetic model of cross section (bottom panel). Top and middle panels show observed and predicted magnetic and gravity variations along the profile. D and S are density and magnetic susceptibility in kg/m^3 and SI units, respectively. If no value for S is given, S equals zero. Note that the geometry of the Oceanic Fault is not constrained by gravity and magnetic data

B

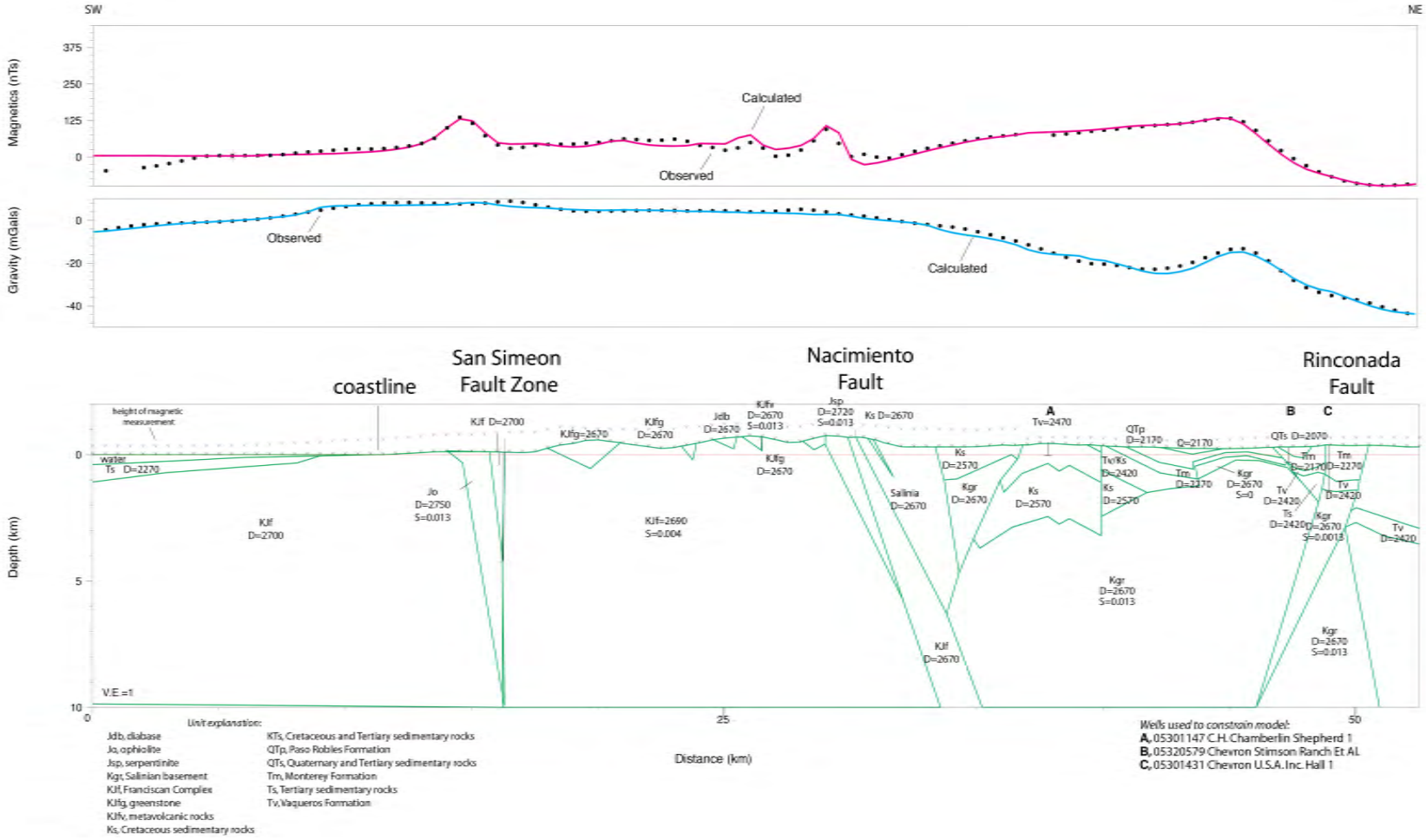

Figure 6.–Continued

In addition to the block-bounding faults, the Piedras Blancas and Santa Lucia Range blocks include the Coast Range Fault, which forms a major basement suture between the parautochthonous Great Valley complex and the allochthonous Franciscan Complex. The Coast Range Fault has a very complex map pattern (fig. 2) resulting from its complicated structural history, including Mesozoic and possible Paleocene subduction and accretion emplacing the terranes of the Franciscan Complex beneath the Coast Range ophiolite, Paleocene(?) and Eocene attenuation faulting associated with thinning of the Great Valley complex and unroofing of the Franciscan Complex, and Oligocene and younger transpressive folding and faulting.

All three blocks also have important Quaternary-active (seismogenic and potentially seismogenic) faults of the San Andreas system, including the Oceanic, Rinconada, and Jolon Faults, and perhaps the Cambria Fault. The Rinconada Fault in the northeast corner of the map area is also thought to be a major block-bounding fault with significant long-term offset (Dibblee, 1976; Graham, 1978), but those relations are not exhibited in the map area because only a few kilometers of the fault trace are found. Finally, numerous lesser faults and folds occur throughout the map area.

Most faults in the map area trend north-northwest, roughly parallel to the Pacific-North American relative plate motion vector (DeMets and others, 2010), giving the topography, including the coastline, a strong north-northwest grain. This grain is cut by three northwest- to west-northwest-trending faults. The Oceanic Fault is known to be an active restraining step in the San Andreas system, transferring slip from the Hosgri-San Simeon Fault Zone to the north-northwest-trending West Huasna Fault southeast of the map area (Hardebeck, 2010). The northern reach of the Nacimiento Fault, as well as a prominent but unnamed fault in the Franciscan Complex, have similar more westerly trends, perhaps reflecting a similar restraining stepover role in a previous period of faulting. Fold axes mostly trend northwest, conjugate to the plate boundary faults.

Earlier workers (Durham, 1968, 1974; Page, 1970) interpreted the Jolon Fault as a major fault extending from its surface trace northwest of Jolon through Lockwood Valley, based on changes in basement depth revealed in petroleum exploration wells and changes in stratigraphy on either side of the fault. However, Dibblee (1976) refuted the existence of the fault beyond its surface trace near Jolon, citing a lack of geomorphic evidence of a fault trace and pointing out that the basement depth and stratigraphic data did not require a fault. Our cross section through Lockwood Valley (fig. 6) shows a reverse fault step in the granitic basement that explains the well and gravity data. Geologic map data are consistent with fault propagation folding over a blind fault, which would not produce the kind of geomorphic expression that Dibblee (1976) was expecting for a fault that ruptured the surface. Therefore, we have remapped the Jolon Fault as a largely blind reverse fault following the maximum horizontal gravity gradient associated with the basement step (fig. 2). Deposits as young as Pleistocene (unit Qoa) are uplifted around a modest topographic high associated with a fault propagation anticline, which we interpret as evidence for Quaternary deformation on the blind fault.

We have also added a reverse fault along the base of the Monterey Formation at Williams Hill, because beds in the Paso Robles Formation (unit QTp) dip toward the contact in multiple places and the presence of older rocks up-dip from younger rocks implies a fault, and the trace of the contact implies a northeast dipping fault. Conversely, we have deleted a previously mapped

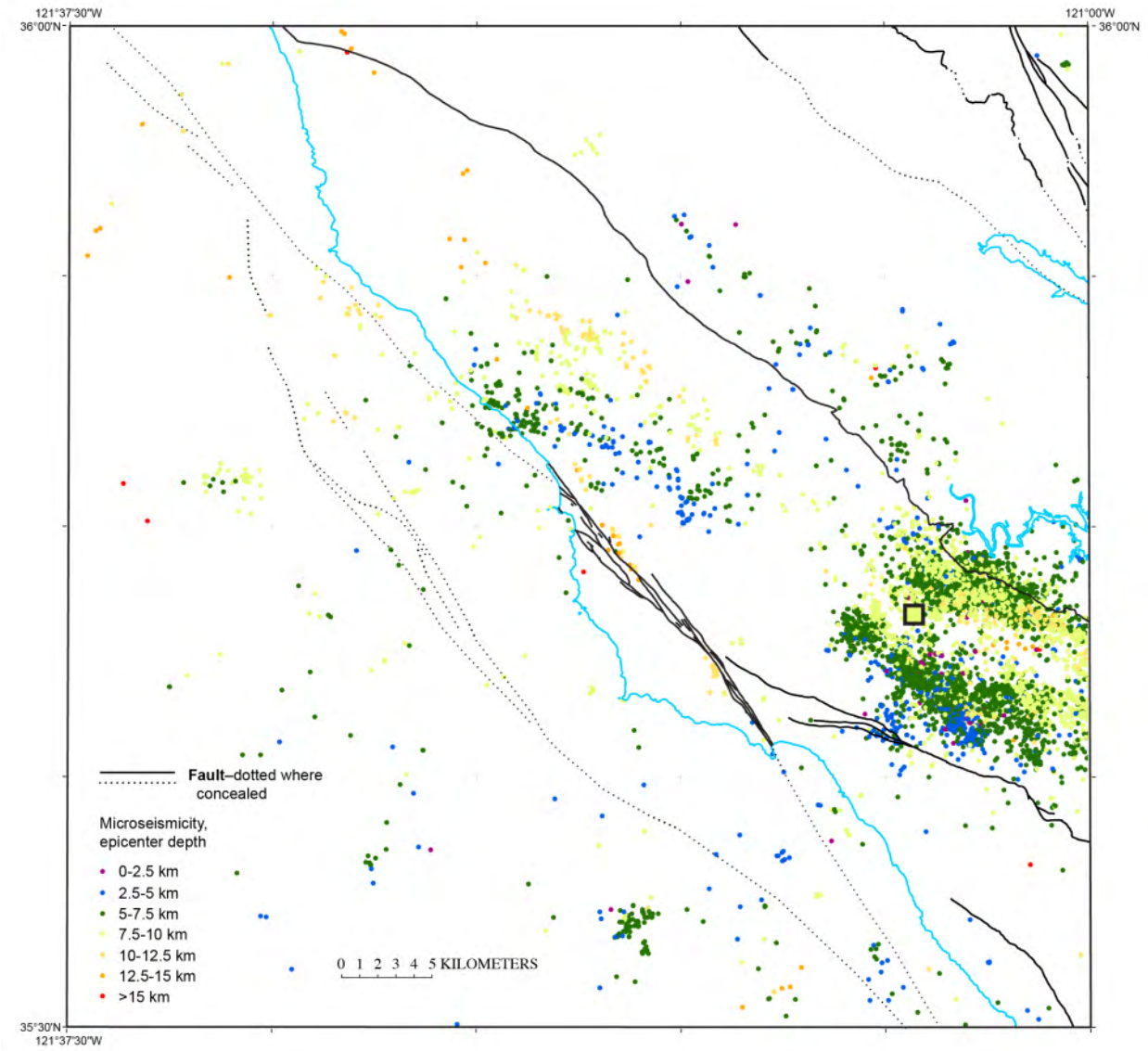

Figure 7. Index map of microseismicity in the map area, color-coded by depth. Double-difference-relocated epicenters from Hardebeck (2010). The 2003 M6.6 San Simeon earthquake epicenter is shown as a black square outline.

strand of the Cambria Fault in the Green Valley area south of Cambria, because new road-cut exposures along Highway 46 clearly reveal a folded depositional contact. The Cambria Fault is considered potentially active because it, or a fault very near to it, was observed by Graymer to juxtapose basement rock with Quaternary gravels in a roadcut on the north side of Main Street in the Santa Rosa Creek valley within the town of Cambria. However the Cambria Fault has little geomorphic expression of fault activity in the Quaternary terraces, so its level of Quaternary activity must be low.

Structural History

The youngest structures in the Cambria region are those related to the San Andreas Fault System. This fault system dominates the Neogene structural history of the map area and, indeed, the entire Coast Ranges. Since about 23 Ma the entire map region has been moved 300–315 km north relative to the Sierra Nevada/Great Valley by offset along the San Andreas Fault (Hill and Dibblee, 1953; Matthews, 1973; Jachens and others, 1998). At the same time, significant offset within and through the map area was accomodated by the Hosgri-San Simeon, Oceanic, and Rinconada Faults.

The San Gregorio-Hosgri Fault System, including the San Simeon Fault Zone, is the main locus of San Andreas Fault System right-lateral strike slip in the map area. The amount of slip on this fault system over the past 30 m.y. diminishes to the south. North of the map area, the San Gregorio-Hosgri Fault System has accumulated about 150 km of right-lateral offset based on correlation of Eocene rock at Point Reyes and Point Lobos (figs. 4*A*, *B*; Clark and others, 1984). Within the map area, the amount of slip is reduced to about 115–130 km, based on correlation of rocks around Point Sur and the Cambria terrane in the map area (Graham and Dickinson, 1978) or rocks at Point San Luis to the south (figs. 4*A*, *B*, Dickinson and others, 2005; Jachens and others, 2009; Langenheim and others, 2013). Studies of thermal maturity suggest that the Mesozoic rocks at Point Sur and Point San Luis were subjected to higher peak temperature than those of the Cambria terrane (Underwood and others, 1995; Underwood and Laughland, 2001), supporting the Point Sur to Point San Luis offset. South of the map area, the slip is reduced to about 90 km, based on correlation of ophiolitic and overlying Tertiary strata around Point Sierra Nevada in the map area and Point Sal to the south (Hall, 1975; Jachens and others, 2009). Near Point Arguello, however, the slip on the fault system is thought to be near zero (Sorlien and others, 1999), consistent with the extent of gravity and magnetic anomalies (Langenheim and others, 2010; 2013). The reduction in slip within the map area from ~150 km to ~120 km has probably been accomplished by partition of ~30 km of slip onto the West Huasna Fault via oblique reverse slip on the Oceanic Fault and possibly other faults (Jachens and others, 2009; Langenheim and others, 2010). A similar partition of about 30 km onto interior faults and compression parallel to the Hosgri Fault is probably present between Point Buchon and Point Sal to account for the decrease from ~120 km to ~90 km. However, the mechanism to account for the reduction of Hosgri Fault slip from ~90 km to ~0 km between Point Sal and Point Arguello is at present unknown. Compressive deformation and oblique reverse slip on the intervening structures is not sufficient to account for more than a few kilometers (Graymer and others, 2010).

The Oceanic Fault is the most recently seismogenic fault in the map area. It generated the 2003 M6.6 San Simeon earthquake (see McLaren and others, 2008, for a detailed study). As mentioned above, the Oceanic Fault connects and transfers slip from the San Gregorio-Hosgri fault system to the West Huasna Fault. Its orientation relative to the Hosgri and West Huasna Faults results in a significant component of reverse (up to the northeast) slip. This connection has been proposed to account for about 30 km of apparent decrease in San Gregorio-Hosgri Fault System offset, but the present-day geometry of the Hosgri-San Simeon and West Huasna Faults (strike about N. 35° W., dip about vertical) and the Oceanic Fault (strike about N. 70° W., dip about 45° NE.) would translate 30 km of Hosgri-San Simeon Fault-parallel horizontal strike slip into roughly 25 km of Oceanic Fault-parallel horizontal strike slip, 24 km of Oceanic Fault-normal reverse slip and 17 km up to the northeast vertical throw, assuming rigid upper crustal blocks. A significant amount of vertical throw is indicated by the presence of coeval plutonic

rocks (unit Td) in the uplifted block and volcanic rocks (unit Tc) in the downthrown block. However, the stratigraphy of the block southwest of the Oceanic Fault shows that it stayed near sea level throughout Neogene time, so, with the footwall elevation roughly constant, reverse throw must have been entirely accomplished by hanging-wall uplift; 17 km is too much, because it would imply rocks in the northeast (hanging-wall) block were uplifted from lower crustal depths, and there are no metamorphic rocks of grade equivalent to that depth present in the block northeast of the Oceanic Fault. This means that the geometry of the faults has changed through time, that a major portion of the 30 km partitioned from the Hosgri-San Simeon has been taken up by some other fault or faults, or that a more complex model of deformation is required. Partition of Hosgri-San Simeon strike-slip would be accommodated with less uplift by an Oceanic Fault more closely subparallel to the Hosgri-San Simeon Fault and (or) with a lower dip. However, folds in the Neogene strata (described below) suggest that the block between the Hosgri-San Simeon and West Huasna Faults has narrowed by compression through the Neogene, so the Oceanic Fault would have been even more orthogonal to the San Gregorio-Hosgri and West Huasna Faults in the past. An average paleo-dip of about 16° (assuming no change in strike) on the Oceanic Fault would yield about 5 km of uplift, which seems reasonable when compared to similar Franciscan Complex lithologies in the hanging wall and footwalls, although the actual amount of hanging-wall uplift is unknown at this time. Alternatively, partitioning only ~10 km of San Gregorio-Hosgri slip onto the Oceanic Fault with present day orientation would result in an equally reasonable ~6 km of hanging-wall uplift, but this would require ~20 km of San Gregorio-Hosgri slip to be taken up by faults to the south. Other faults that could have transferred part of the 30 km between the San Gregorio-Hosgri and West Huasna Faults include the Cambria Fault and, south of the map area, the Los Osos Fault. A third alternative is that the upper crust did not deform as rigid blocks. Down-bending of the footwall beneath the fault would allow some of the vertical throw to be accomplished by downward motion of the footwall while maintaining the portion of the footwall block south of the fault near sea level.

The Rinconada Fault crosses the extreme northeast corner of the map area. Rosenberg and Clark (2009) estimate that it has about 38 km of Miocene and younger right-lateral offset based on correlated granitic rocks, 18 km of which is thought to have accumulated since the early Pliocene. This fault cuts Pleistocene alluvial gravels near Paso Robles (Rosenberg and Clark, 2009), east of the map area, but there is no definitive evidence of Holocene offset, and the fault is not seen to cut overlapping colluvium in trenches.

Other Neogene and Quaternary structures, including the Jolon Fault, mostly accommodate significant southwest-northeast shortening. Out-of-plane slip on strike-slip faults and lateral pinch-out of various horizons within structural blocks preclude calculation of shortening across the whole map area, but Tertiary southwest-northeast shortening of about 21 percent within the San Antonio block is measured using the base of the Vaqueros Sandstone in cross section (fig. 6).

The Nacimiento Fault forms the boundary between Salinian complex basement on the northeast and Franciscan Complex/Great Valley complex composite basement on the southwest. At the eastern edge of the map, this fault cuts middle Miocene Monterey Shale, showing that some part of its activity extended into Miocene time. Microearthquakes (Hardebeck, 2010) form a diffuse band parallel to and slightly northeast of the mapped Nacimiento Fault for nearly a distance of 25 km (fig. 7). The trend of the Nacimiento seismicity is slightly more northerly than that of the main band of aftershocks of the 2003 San Simeon earthquake. Stress from the San Simeon earthquake may have triggered minor slip on a number of faults in the region northeast

of the Nacimiento Fault, including the Nacimiento Fault itself. Microearthquakes also occurred in this band before the 2003 mainshock. Note, however, that the southwest-dipping backthrust that ruptured in the 2003 earthquake cut the Nacimiento Fault (McLaren and others, 2008) where the Oceanic and Nacimiento Faults merge, approximately 10 km to the southeast of the Cambria quadrangle.

The original subduction zone contact between the inboard (hanging wall) Great Valley complex and the accreting (footwall) Franciscan Complex has been overprinted everywhere in the map area by attenuation (normal) faults associated with the unroofing of the Franciscan Complex, similar to most parts of the Coast Ranges (Krueger and Jones, 1989; Harms and others, 1992). In the map area, high-grade Franciscan Complex metamorphic rocks are juxtaposed against the unmetamorphosed rocks of the Great Valley complex, and the Coast Range ophiolite at the base of the Great Valley complex is significantly thinned. This attenuation faulting must have occurred after accretion of the Late Cretaceous (Campanian) Cambria terrane but prior to emplacement of the unnamed Oligocene(?) dacite (unit Td), which intrudes the fault contact near Pine Mountain east of San Simeon. In the Coast Ranges east of the San Andreas Fault, attenuation and unroofing of Franciscan Complex rocks was at least locally complete by Paleocene-Eocene time because Franciscan Complex detritus is found in Paleocene-Eocene strata overlying Great Valley complex strata in Rice Valley (Berkland, 1973) and New Idria (Dibblee and Nilsen, 1977). Pre-Oligocene Tertiary strata are not present in the part of the map area underlain by Franciscan Complex rocks, so the timing of attenuation and unroofing is not as tightly constrained.

Salinian complex basement was rapidly uplifted in Late Cretaceous time. Radiometric dating of granitic rocks just north of the map region (Kistler and Champion, 2001) show that the basement was at depth as recently as 78.2 Ma. By the Maastrichtian (70.6–65.5 Ma) the basement was present at the surface and overlain by sedimentary rocks.

The Salinas Shear Zone, which places the Salinian complex over the Cretaceous schist of Sierra de Salinas, does not crop out in the map area but presumably underlies all of the San Antonio block at significant depth. This regional thrust fault is highly deformed by folding and faulting but is thought to have been originally a shallowly east-dipping fault (Hall, 1991; Barth and others, 2003; Ducea and others, 2009). The schist has yielded detrital zircons suggesting a depositional age for the protolith of about 79 Ma (Ducea and others, 2009), so thrusting must have initiated after that time. Kidder and Ducea (2006) calculated thermobarometric measurements as much as 714°C and 13.7 kbar for the schist. $^{40}Ar/^{39}Ar$ dating of metamorphic muscovite in the schist of Sierra de Salinas suggests subsequent cooling to ~350°C by about 71 Ma, and biotite $^{40}Ar/^{39}Ar$ dating of the schist reveals that it had been cooled to about 250°C by about 70 Ma (Barth and others, 2003), probably reflecting partial uplift by that time (Ducea and others, 2009). So peak metamorphism and maximum underthrusting must have occurred between 79–72 Ma (Barth and others, 2003; Ducea and others, 2009). It is tempting to equate the underthrusting of the schist with the similarly timed uplift of Salinian complex basement, but Ducea and others (2009) show that similar cooling histories for the schist and granitic rocks suggest that much of the granite uplift postdated underthrusting and that the schist and Salinian complex granitic/metamorphic basement were uplifted very rapidly between about 75–68 Ma.

The oldest structures in the map area are those related to Jurassic (?) and Cretaceous subduction and accretion of Franciscan Complex rocks. These structures have largely been reactivated, deformed, and otherwise obscured by subsequent tectonic periods, but these early faults may be preserved in places as mélange-block bounding faults and faults between mélange

and relatively coherent terranes. The interpretation of Late Cretaceous sandstone of the Cambria terrane as trench-basin sediments suggests that subduction was ongoing 90–80 Ma.

DESCRIPTION OF MAP UNITS

[BFS, benthic foraminiferal stage; CPMS, California provincial molluscan stage]

Unit descriptions are divided into three sections. The first section describes Quaternary surficial deposits that are similar throughout the map area. The second section describes early Pleistocene and Tertiary strata and is subdivided into three sections based on areas of structural blocks which display a relatively consistent stratigraphy (fig. 2). As noted above, fault offset within the map area has juxtaposed depositional basins or parts of depositional basins that were once kilometers or tens of kilometers apart, therefore the stratigraphy in adjacent assemblages may be quite different. It is also important to note that units of similar stratigraphic position in various parts of the map area have been traditionally given the same unit name, despite differences in lithology or age. Therefore, each stratigraphic unit is described in each assemblage, even if a unit has the same name as one already described for another assemblage. The third section describes rocks of the Mesozoic and Paleogene basement complexes that underlie Tertiary strata.

QUATERNARY SURFICIAL DEPOSITS

Qs **Beach and dune sand (Holocene)**—Fine-grained, very well sorted, well-drained, eolian and shoreline deposits

Qal **Alluvial fan and fluvial deposits (Quaternary)**—Alluvial fan deposits are brown or tan, medium dense to dense, gravelly sand or sandy gravel that generally grade upward to sandy or silty clay. Near distal fan edges, fluvial deposits are typically brown, medium dense sand that fines upward to sandy or silty clay. Floodplain deposits are medium to dark gray, dense, sandy to silty clay, locally with lenses of coarser material (silt, sand, and pebbles). Natural levee deposits consist of loose, moderately sorted to well-sorted sandy or clayey silt grading to sandy or silty clay. They are porous and permeable and provide conduits for transport of ground water. Levee deposits border stream channels, usually both banks, and slope away to flatter floodplains. Stream-channel deposits consist of poorly sorted to well-sorted sand, silt, silty sand, or sandy gravel with minor cobbles. Cobbles are more abundant in mountain valleys

Qls **Landslide deposits (Quaternary)**—Poorly sorted clay, silt, sand, gravel, boulders, and rock masses. Only a few large landslides are shown. Includes all levels of activity (dormant to active)

Qoa **Older alluvium (Pleistocene)**—Roughly horizontal beds of buff siltstone and claystone, buff to gray fine- to coarse-grained lithic sandstone, pebbly sandstone, pebbly mudstone, and pebble to cobble conglomerate. These deposits lie above the present alluvial level and are typically more consolidated and dissected by erosion

Qt **Fluvial terrace deposits (Pleistocene)**—Underlies small areas on Williams Hill and along San Antonio River. Deposits consist of crudely bedded, clast-supported gravels, cobbles, and boulders with a sandy matrix. Clasts as much as 35 cm

intermediate diameter are present. Coarse sand lenses may be locally present. Fluvial terrace deposits rest on flat surfaces cut a few meters into bedrock. These surfaces are up to several tens of meters above Qal deposits. Terrace deposits are remnants of an older alluvial system that have been tectonically uplifted above present depositional levels

Qmt **Undifferentiated marine terrace desposits (Pleistocene)**—Largely composed of unconsolidated sand and gravel. Marine terraces are geomorphically expressed as gently seaward sloping surfaces. Deposits include older beach and nearshore sediments typically capped by younger aeolian and alluvial sediments. Sediments are underlain by a wave-cut bedrock platform that is rarely exposed. Though there may be several distinct terraces within this unit, only the more prominent surfaces have been differentiated for this study (see below). These surfaces are treated as geomorphic surfaces; in many places, terrace-cover sediments such as sand dunes are included in the unit descriptions

Qmtss **San Simeon terrace (Late Pleistocene)**—Lowest emergent terrace in the San Simeon area, consisting of a wave-cut platform and overlying sediments. Thermoluminescence and uranium-series dating methods reveal the terrace formed during a sea-level highstand at 105 ka or 80 ka (Hanson and others, 1994). The San Simeon terrace is discontinuous north of Cambria and either absent or indistinguishable from the modern wave-cut platform south of Cambria (Weber, 1983). A lower, narrower, discontinuous step along the southwest side of San Simeon Point has been designated the “Point Terrace” by others (Hanson and others, 1994; Rockwell and others, 1987); it is not found elsewhere in the mapped area and appears to merge with the San Simeon platform

Qmttr **Tripod terrace (Late Pleistocene)**—An extensive wave-cut platform and overlying sediments situated 3–6 m (10–20 ft) above the San Simeon terrace. Occasionally the step between the San Simeon and Tripod terraces is buried by alluvial fans or talus, giving the appearance of one broad terrace surface (Weber, 1983). Between Cambria and Point Estero, the terrace becomes a very narrow, irregular surface with sporadic old sea stacks. Weber (1983) suggests the Tripod terrace is a continuation of the Cayucos terrace mapped south of the map area. The Cayucos terrace has been dated at 120 ka using amino acid racemization of fossils. Assuming the terraces are correlative, the Tripod terrace was formed during the 120 ka sea-level highstand, when sea level was approximately 6 m higher than present

Qmtos **Oso terrace (Middle Pleistocene?)**—Originally mapped by Weber (1983) as a thin, discontinuous marine-terrace surface only observed north of San Simeon Fault Zone. A later study (Hanson and others, 1994) identified remnants of the Oso terrace south of the fault. However, this correlation is tentative, as the Oso terrace is located in an area of complex faulting. Weber (1983) calculated a local tectonic uplift rate of 0.65 ft/k.y. based on the age of the Tripod terrace. Assuming this rate is correct, the Oso terrace would have formed during the 310 ka sea-level highstand

Qmtlc **La Cruz terrace (Middle Pleistocene)**—This marine terrace is best developed

northeast of Point Piedras Blancas; elsewhere, it is thin and discontinuous. A large portion of the terrace appears to have been stripped of marine sediments and is now overlain by a veneer of fluvial sediments (Hanson and others, 1994). Using the assumed local tectonic uplift rate of 0.65 ft/k.y., the La Cruz terrace can be correlated to a 340 ka sea-level highstand (Weber, 1983)

Qmtcm **Cambria terrace (Middle Pleistocene)**—A well-developed terrace surface often covered by a thick package of sediments. The Cambria terrace may include multiple platforms, though thick aeolian cover makes distinguishing individual surfaces difficult (Weber, 1983). If the local tectonic uplift rates calculated from the age of the Tripod terrace have been constant, the Cambria terrace would correlate to a 540 ka or older sea-level highstand (Weber, 1983). Dissection of the terrace is not consistent with this age, so the Cambria terrace is more likely correlative to a 340 ka sea-level highstand, though that would require a change in uplift rate to 1.1 ft/k.y. (Weber, 1983). The lower portion of the terrace may be correlative to the La Cruz terrace described above; the upper surface may merge with either Scott Rock or Del Puerto terraces (Weber, 1983) described below

Qmtdp **Del Puerto terrace (Middle Pleistocene)**—Consists of a few scattered terrace remnants situated between the northern and southern strands of Oceanic Fault. This terrace may include two wave-cut platforms, though poor exposure makes this interpretation difficult to verify (Weber, 1983). It is possible that the lower portion of the terrace may merge with an upper surface of the Cambria terrace. If so, the Del Puerto terrace would have formed during the same 340 ka sea-level highstand as the Cambria terrace

Qmtbb **B.B. terrace (Middle Pleistocene)**—A few small remnants located between the northern and southern strands of Oceanic Fault, near Broken Bridge Creek. These surfaces are 50–100 ft higher than the Del Puerto terrace. There is no definitive correlation of the B.B. terrace with other terraces; if a local uplift rate of 0.98 ft/k.y. is applied for the mid-Pleistocene, the terrace may have formed during the 430 ka sea-level highstand (Weber, 1983)

Qmtsr **Scott Rock terrace (Middle Pleistocene)**—Preserved in scattered remnants near Scott Rock north of Cambria. Terrace surfaces are often covered by aeolian sands. South of San Simeon Creek, the Scott Rock terrace nearly merges with the upper part of the Cambria terrace (Weber, 1983). The age of the terrace is unknown; if the same uplift rate estimated for the Cambria terrace is used (~1.1ft/k.y.), the Scott Rock terrace may correlate to a 430–415 ka sea-level highstand (Weber, 1983)

Qmtok **Oak Knoll terrace (Middle Pleistocene)**—Forms uplands in the Piedras Blancas structural block. Terrace surface is best expressed near Oak Knoll, and includes old sea stacks and sand dunes. Based on its elevation, it must be at least slightly older than the La Cruz terrace, but younger than the Cinnabar terrace

Qmtcb **Cinnabar terrace (Middle Pleistocene)**—Scattered terrace remnants forming the highest uplands in Piedras Blancas structural block (Weber, 1983). Extensively faulted and deformed, and in several areas eroded to a bedrock platform covered by thin lag deposits (Weber, 1983). Using an estimated

uplift rate of 1.6 ft/k.y. (based on the best fit with the sea-level fluctuation curve), the Cinnabar terrace could have formed during a 435 ka sea-level highstand and may correlate with the Scott Rock terrace (Weber, 1983)

Qmtvg **Van Gordon terrace (Middle Pleistocene)**—Scattered terrace remnants that manifest as topographic benches and flats south of San Simeon. Using the local uplift rate estimated for the Cambria terrace (~1.1ft/k.y.), the Van Gordon terrace would correlate to the 590–520 ka sea-level highstand (Weber, 1983)

EARLY QUATERNARY AND TERTIARY STRATA

PIEDRAS BLANCAS BLOCK

Ts **Unnamed sandstone and conglomerate (Pliocene)**—Gray and greenish-gray fossiliferous pebble to cobble conglomerate and buff-weathering greenish-gray lithic sandstone. Conglomerate clasts include laminated siliceous mudstone, laminated chert, argillite, greenstone, greenish wacke, black chert, serpentinite, and vesicular andesite. Shell bits are common sand grains. Mollusk fossils include Pectinid bivalves, *Anadara*, oysters, and various gastropods. Hall (1976) also reports the echinoderm *Dendraster*, indeterminate bryozoans, the Scaphopod mollusk genus *Dentalium*, and the bivalve mollusk genera *Nuculana* and *Solen*. This unit was correlated with the Graciosa member of the Careaga Sandstone in the Santa Maria area by Hall (1975) based on lithologic similarity

Tm **Monterey Formation (late Miocene)**—Laminated white, brown, and black chert, diatomite, diatomaceous shale, porcelanite, porcelaneous shale, siltstone, and cherty shale. Foraminifers from the unit near San Simeon Point are reported to be late Miocene (Malmblorg and others, 2008).

The Monterey Formation in the Piedras Blancas block differs from that in the adjacent Santa Lucia Range block by the absence of significant volcanic rocks at the base and its younger age. It differs from that of the San Antonio block by its limited thickness and lack of early and middle Miocene strata at the base

Tl **Lospe Formation (early Miocene)**—Sedimentary and minor volcanic rocks. The Lospe Formation in the Piedras Blancas block was mapped as Oligocene by Hall (1976), but correlative Lospe Formation in the Point Sal region is now known to be Lower Miocene based on microfossils and radiometric dating of interbedded volcanic rocks (Stanley and others, 1990, 1996). Preliminary detrital zircon data indicate that the maximum age of the Lospe Formation in the Piedras Blancas block is also Lower Miocene (17.9±0.9 Ma; J.P. Colgan, written commun., 2011). In the Piedras Blancas block this unit largely consists of gray, red, and green sandstone and conglomerate. Clasts are mostly ophiolite.

The Lospe Formation in the Piedras Blancas block differs from that in the adjacent Santa Lucia Range block by its younger age, clast composition, and inclusion of volcanic rocks

SANTA LUCIA RANGE BLOCK

QTcs **Sedimentary rocks of Crystal Knob (Pleistocene or Pliocene)**—Poorly consolidated nonmarine gray-green sandstone and conglomerate. Clasts angular to rounded, including ophiolite, Franciscan Complex rocks, and minor basalt of Crystal Knob. Outcrop limited to a roughly circular area about 700 m in diameter. Presumably deposited in a volcanic depression (Seiders, 1989a). The age of the unit is poorly constrained but suggested to be post-early Pliocene by preserved volcanic geomorphology and weak consolidation

QTcb **Basalt of Crystal Knob (Pleistocene or Pliocene)**—Dark-gray olivine basalt, in part vesicular. Crops out as a lens within unit QTcs

Pismo Formation (early Pliocene and late Miocene)

Tpm **Mudstone member**—White and lesser light-brown claystone, siltstone, sandy mudstone, diatomite, diatomaceous shale, porcelanite, porcelaneous shale, and chert

Tps **Sandstone and conglomerate member**—Light-brown and orangish-brown fine- to medium-grained arkose and pebble and cobble conglomerate. Conglomerate clasts include felsite (probably derived from unit Tc) and varicolored chert (probably derived from Franciscan Complex chert). Hall (1974) reports Mohnian or Delmontian(?) benthic foraminiferal stage (BFS) fossils from this unit

Tm **Monterey Formation (early and middle Miocene)**—White-weathering dark-brown siliceous shale, porcelaneous shale, chert, claystone, siltstone, tuffaceous siltstone, and minor sandstone, in most places laminated. Locally contains orange-weathering dolomitic concretions. Flaggy outcrop common. Previously mapped in part as Rincon Shale (Hall, 1976). Fossils reported by Hall (1974) from the map area suggest Saucesian or Relizian BFS (early or early middle Miocene) age. More definitive foraminfera reported from this unit to the east (Seiders, 1982) are the same age. At its base in much of the map area and to the east, the Monterey Formation also includes a volcanic member

Tmv **Monterey Formation, volcanic member**—Diabase and basalt sills and flows, and white to gray hard microcrystalline tuff.

The Monterey Formation in the Santa Lucia Range block differs from that in the San Antonio block by its limited thickness, lack of late Miocene strata, and the presence of significant volcanic rocks at the base

Tv **Vaqueros Sandstone (early Miocene and late Oligocene?)**—White medium- to coarse-grained lithic arkose. Includes shell hash locally and cobble-boulder conglomerate at the base. Locally glauconitic. Conglomerate clasts include rhyolite and dacite (probably derived from the underlying Cambria Felsite) and lesser varicolored chert, graywacke, and blueschist (probably derived from the underlying Franciscan Complex). Mega-fossils include the bivalve mollusk families Ostreidae and Pectinidae and indeterminate barnacles (see Hall, 1974, for a detailed list) reported to be Oligocene. Hall (1974) lists these fossils as “Zemorrian”, but that is an Oligocene benthic foraminiferal stage (BFS). We interpret that to mean that the mollusks should be assigned to the early “Vaqueros” California provincial molluscan stage (CPMS). In contrast,

Malmblorg and others (2008) report early Miocene, late Miocene, and two Miocene, possibly pseudosaucesian facies, foraminifer localities. Strata previously assigned to the “Vaqueros” CPMS vary widely in age (Hoffman and others, 2001; Prothero and Hoffman, 2001) but the “Vaqueros” CPMS appears to span late Oligocene and early Miocene (28–17 Ma; Prothero and Donohoo, 2001). The “early Miocene” foraminiferal age assignment implies the correlation with the Saucesian BFS. The “Miocene, possibly pseudosaucesian facies” age interpretation could not be verified but indicates a deepwater assemblage of Miocene age, Saucesian BFS or younger. The “late Miocene?” assemblage was examined and contains a single species which ranges from Oligocene (coeval with planktic foraminiferal zone P20) through Pleistocene (planktic foraminiferal zone N23). However, the age of the overlying Monterey Formation precludes assignment of an age younger than early Miocene to this unit. All together these fossil and stratigraphic data imply a possibly late Oligocene to early Miocene age.

The Vaqueros Sandstone of the Santa Lucia Range block differs from that of the San Antonio block in the presence of Franciscan Complex and Cambria felsite detritus rather than Salinian complex detritus found in the Vaqueros Sandstone of the San Antonio block

Tls **Limestone (early Miocene or Oligocene?)**—Thick-bedded, light-gray, coarse-grained, bioclastic limestone and calcareous sandstone. Locally contains pebbles and cobbles of felsic volcanic rocks. Contains large mollusks of “Vaqueros” CPMS (early Miocene and late Oligocene; Prothero and Donohoo, 2001), as well as early Miocene foraminifers just to the east of the map area at Lime Mountain (Malmblorg and others, 2008). In the map area this unit only has a small outcrop at the eastern edge of the map area between 35°37'30"N and 35°45'N

Tl **Lospe Formation (Oligocene)**—Maroon weathering, red, green, and greenish-gray lithic sandstone, mudstone, and pebble to cobble conglomerate. Clasts include varicolored chert and graywacke (probably derived from the underlying Franciscan Complex), plagioclase porphyry (probably derived from the underlying Cambria felsite), quartz, and lithic sandstone. Nonmarine. Note that the Lospe Formation here is considerably older than that in the Piedras Blancas block

Tc **Cambria Felsite (Oligocene)**—White, welded, vesicular feldspar-quartz-pumice tuff; laminated, thick-bedded quartz-feldspar-biotite tuff (some euhedral biotite); and white and gray, hard rhyolite and dacite felsite. East of the map area (Cypress Mountain 7.5´ quadrangle), in roadcuts along Highway 46, this unit also includes black-weathering maroon amygdaloidal basalt with green serpentinite(?) xenoliths and green mineralization, white-weathering green tuff including lenses of silicified breccia, obsidian and flow-banded gray glassy rhyolite, and greenish-gray tuff breccia with boulders of red jasper. See Ernst and Hall (1974) for a detailed description of this unit. The felsite has been correlated with the Morro Rock-Islay Hill intrusive/volcanic complex southeast of the map area (Ernst and Hall, 1974), which has yielded K-Ar ages between 22.7±0.9 and 28.0±1.0 Ma (Turner, 1968; Hall and others, 1966;

Buckley, 1986) and more recently an $^{40}Ar/^{39}Ar$ age of 26.5–27 Ma (cited in Cole and Stanley, 1998). Ernst and others (2011) used U-Pb ages from zircons to date Cambria Felsite at 27 Ma. The Oligocene age is consistent with stratigraphic position beneath the fossiliferous Vaqueros Sandstone and correlation with the Oligocene rocks to the southeast

Td **Dacite (Oligocene?)**—Gray to white, porphyritic-aphanitic dacite. Crops out as small intrusive bodies within Franciscan Complex and Coast Range ophiolite basement northeast of the Oceanic Fault. Tentative age based on correlation with the Oligocene Morro Rock-Islay Hill complex (Hall, 1976) southeast of the map area (see description of unit Tc above)

SAN ANTONIO BLOCK

QTp **Paso Robles Formation (Pleistocene and (or) Pliocene)**—Southwest of San Antonio River, this unit is made up of white-weathering, light-gray, light-brown, and yellowish-green arkose and K-spar arkose, pebbly-cobbly sandstone, and pebble to cobble gravel. Clasts include granitic rocks, red to white rhyolite, green plagioclase porphyry, red chert, black cherty argillite, sandstone, laminated shale, and brown mudstone. On the northeast margin of Lockwood Valley, this unit is made up of angular to well-rounded pebble to cobble conglomerate. Clasts are almost all porcellanite and siliceous shale derived from Monterey Formation (Tm), which underlies the adjacent uplands. This unit is nonmarine in both places

Tu **Unnamed sandstone (early Pliocene and late Miocene?)**—Buff-weathering light-gray sandstone. Chiefly distinguished by early Pliocene or, in places, possibly late Miocene mollusks, roughly equivalent to those of the Pancho Rico Formation east of the map area (Durham, 1974)

Tm **Monterey Formation (Miocene)**—White-weathering, thin-bedded, flaggy, brown, gray, and black, laminated in places foraminiferal mudstone, siliceous shale, porcellanite, and chert. Locally, also includes minor orange dolomitic mudstone, fine-grained arkose, and sandy shale. Sparse mollusk fossils have been found. Foraminifers southwest of San Antonio River range from late Saucesian BFS to late Mohnian BFS (early to late Miocene), whereas those in the Williams Hill area are late Mohnian BFS (late Miocene) in age (refer to paleontological data files)

Tv **Vaqueros Sandstone (early Miocene and (or) late Oligocene)**—White-, brown-, or gray-weathering, gray quartz sandstone and arkose. Locally includes lithic arkose, pebble to boulder conglomerate, shell hash, and thin beds of gray and brown claystone, silty claystone, and siltstone. Coarse clasts dominantly granitic, with lesser quartzite and andesite. “Vaqueros” CPMS (late Oligocene and early Miocene; Addicott, 1976) mollusk fossils are common (Loel and Corey, 1932; Durham, 1974). Vaqueros Sandstone strata in this block north of the map area are known to be Oligocene (Addicott, 1979), but Saucesian BFS (early Miocene) foraminifera are reported from this unit in the eastern part of the map area (Malmblorg and others, 2008; new data, refer to paleontological data files)

BASEMENT COMPLEXES

SALINIAN COMPLEX

Tpa **Piedras Altas Formation (Paleogene)**—Red, red-gray, and greenish-gray nonmarine sandstone, pebbly sandstone, and conglomerate. Conglomerate is poorly sorted, with subangular to well-rounded pebbles, cobbles, and sparse boulders; clasts are mainly felsic volcanic and granitic rocks and arkose. The age of this unit is based on its stratigraphic position conformably over the Shut-in Formation and unconformably beneath the Vaqueros Sandstone. We interpret the angular unconformity above the Salinian complex basement to represent considerable time and note that the Piedras Altas Formation is relatively thin; therefore, we suggest that the age of this unit is likely restricted to the Paleocene and possibly the early Eocene. This interpretation is supported by relations north of the map area where the equivalent angular unconformity lies between Paleocene and late Paleocene to Eocene strata (Graham, 1979)

TKsi **Shut-in Formation (Paleocene and latest Cretaceous, Maastrichtian)**—Gray, marine sandstone, mudstone, and conglomerate. Clasts are felsic volcanic and granitic rocks. This unit has yielded Maastrichtian (Seiders, 1989a) and Paleocene (Durham, 1965; see also new data in paleontological data files) foraminifers in the map area

TKsic **Shut-in Formation, conglomerate and sandstone member**—Thick-bedded conglomerate, sandstone, and pebbly sandstone

Kif **Italian Flat Formation (latest Cretaceous, Maastrichtian)**—Thick-bedded gray marine sandstone, gritstone, and pebbly sandstone. Subordinate thin- to medium-bedded sandstone and mudstone. In the map area, has yielded Maastrichtian pollen and dinoflagellates (Butler, 1984)

Ksc **Steve Creek Formation (latest Cretaceous, Maastrichtian)**—Thin- to thick-bedded, marine, greenish-gray sandstone and olive-gray mudstone with local conglomerate. Sandstone includes white- and buff-weathering quartz-lithic and quartz-biotite-lithic wacke. This unit has previously been assigned to the Campanian(?), but its position between two Maastrichtian units precludes that interpretation

Kscc **Steve Creek Formation, conglomerate and sandstone member**—Thick-bedded pebble to boulder conglomerate and subordinate sandstone. Clasts mainly felsic volcanic rocks with lesser intermediate and mafic volcanic, sedimentary, and granitic rocks

Kep **El Piojo Formation (latest Cretaceous, Maastrichtian)**—Gray marine sandstone and mudstone with minor conglomerate. Sandstone chiefly thick-bedded, coarse-grained, brown- or white-weathering biotite and biotite-lithic arkose, locally pebbly or cobbly. Lesser thin-bedded, brown-weathering, fine-grained, laminated biotite-lithic arkose and mica mudstone and white-weathering, yellow-brown, muscovite-biotite siltstone. The El Piojo has yielded Maastrichtian, as well as long-ranging Late Cretaceous to Paleogene foraminifera (Seiders, 1989a; see also new data in paleontological data files)

Kepc **El Piojo Formation, conglomerate member**—Thick-bedded conglomerate. Clasts mostly felsic volcanic and granitic rocks. Sparse interbedded sandstone.

Crops out as discontinuous lenses in the northwest part of the formation

Ku **Unnamed strata (latest Cretaceous, Maastrichtian)**—Brown and white arkose and lithic sandstone, pebbly to bouldery arkose and pebble to boulder conglomerate, and brown, gray, and dark-greenish-gray mudstone and shale. Unconformable contact on granitic and metamorphic basement was observed by us in the northern part of the map area. Mudstone in the map area locally includes foraminifera of long-ranging (Late Cretaceous to Eocene) arenaceous species (see paleontological data files). However, the age of overlying strata and isotopic data from the underlying basement (Mattinson, 1978; Ducea and others, 2009) constrain the age of the unit to Maastrichtian (latest Cretaceous)

Km **Sur series metamorphic rocks and granitic rocks, undifferentiated (Cretaceous)**—Quartz-feldspar and hornblende gneiss, biotite schist, marble, and biotite quartz diorite. There are no age data from the map area for this unit, but Barbeau and others (2005) inferred a maximum age of protolith deposition of 280 Ma and 360 Ma for two Sur series samples collected just north of the map area in the Cone Peak 7.5´ quadrangle. Isotopic dates (Mattinson, 1978; Kistler and Champion, 2001) from a pluton (charnokitic tonalite of Compton, 1960) in the same structural block about 20 km north of the map area suggest pluton emplacement about 100 Ma (zircon U-Pb, Rb-Sr whole rock) and thermal overprint (Kistler and Champion, 2001) or rapid partial uplift (Mattinson, 1978) between about 84 and 76 Ma (hornblende and biotite $^{40}Ar/^{39}Ar$, Rb-Sr). Other plutonic rocks farther north have yielded ages around 83.5 Ma (quartz diorite of Soberanes Point) and 117 Ma (granodiorite-quartz diorite of Junipero Serra Peak, Rb-Sr whole rock, Kistler and Champion, 2001), so we interpret the age of plutonic rocks in the map area to be within the span of 83.5–117 Ma

Kmm **Sur series metamorphic rocks, marble member**—Blue-gray weathering, white crystalline marble

FRANCISCAN COMPLEX

Kfm **Mélange (Late Cretaceous)**—Sheared black and gray argillite enclosing blocks of graywacke, conglomerate, greenstone, diabase, chert, serpentinite, and glaucophane schist ranging in size from pebble to hill-sized. Sheared matrix has yielded Early Cretaceous (probably Albian) spore and dinoflagellate fossils (Page, 1970). Chert blocks have yielded Early or Middle Jurassic to Early Cretaceous radiolarians (Seiders, 1989a,b). Chert pebbles in conglomerate blocks have yielded Late Triassic to Late Jurassic radiolarians. Some graywacke blocks in the Santa Lucia Range block have detrital zircons yielding a maximum depositional age of 90–77 Ma (Morisani and others, 2005). The mélange probably formed by tectonic interleaving and mixing of accreted terranes at the subduction margin along the western edge of the North American plate. Initiation of this mixing must postdate the Early Cretaceous fossils in the matrix, and mixing must have extended past the age of Late Cretaceous zircons and fossils in enclosed graywacke blocks and the Cambria terrane (see below). Note that the presence of Late Cretaceous blocks in an Early Cretaceous matrix precludes an olistostromal origin for the mélange in

the map area

Cambria terrane

Kfg **Sandstone of Cambria (Late Cretaceous)**—Medium- to thick-bedded, red-orange weathering, pink and light-gray, medium-grained arkose; yellow-brown-weathering, thin-bedded to massive, in places laminated, medium- to light-gray, fine- to coarse-grained arkosic wacke; and gray biotite-lithic wacke. Locally, sandstone grains include much carbon debris. Sandstone beds separated in places by thin beds of medium-gray biotite-carboniferous mudstone and sandy mudstone and sheared dark-gray shale, which locally contain Late Cretaceous foraminfera and pollen. This unit has also yielded detrital zircons of about 80–90 Ma (Jacobson and others, 2011)

Unnamed Disrupted Terrane(s)

KJfg **Sandstone (Cretaceous and Jurassic?)**—Medium-bedded to very thick bedded, brown-weathering, greenish-gray, green, and gray biotite-lithic wacke and biotite arkosic wacke and attenuated thin interbeds of medium-dark-gray fine-grained wacke, siltstone, claystone, and minor coal. Shale chips are common sand grains. Locally includes conglomerate and pebbly shale. This unit crops out as large fault-bounded slabs and blocks in mélange. U-Pb dates from detrital zircons in graywacke near San Simeon yielded maximum ages of deposition between 90 and 77 Ma (Late Cretaceous; Morisani and others, 2005), younger than fossils in the mélange matrix but roughly coeval and perhaps equivalent to sandstone of Cambria slab, although the two units differ in sandstone composition. Graywacke elsewhere in the map unit is undated and may differ from any of the other Franciscan sandstones. Franciscan Complex Central Belt graywackes are known to be as old as Jurassic (Blake and Jones, 1974; Murchey and Jones, 1984), although the presence of Early Cretaceous fossils in the chert and the model of graywacke over chert deposition (See Basement Complexes section under Stratigraphy) makes a Jurassic age for any part of this unit questionable

KJfb **Broken formation (Cretaceous and Jurassic?)**—Structurally disrupted graywacke and shale and schistose metagraywacke and slate. Locally includes minor blocks of chert, metachert, and basalt. In outcrop, unfoliated graywacke and shale are indistinguishable from unit KJfg but entirely lacking coherence at scales more than a few meters, resulting in a unit more resembling the block in matrix texture of unit Kfm but distinguished by the lack of exotic blocks and a paucity of chert and basalt

KJfc **Chert (Cretaceous and Jurassic)**—Red and green ribbon chert with very thin shale partings and white and gray metachert with slate partings. Crops out as blocks and lenses in units Kfm and rarely in KJfb, many too small to show at map scale. This unit has yielded Early or Middle Jurassic to Early Cretaceous radiolaria in the map area (Seiders, 1989a,b)

KJfv **Mafic volcanic rocks (Cretaceous? and Jurassic)**—Orange-weathering, black, dark-gray, and green basalt, pillow basalt, basalt breccia, basaltic tuff, and diabase. Basalt is locally amygduloidal. Crops out as blocks and lenses in units Kfm and rarely in KJfb, many too small to show at map scale. This unit

is entirely without fossil or radiometric age data. Franciscan Complex volcanic rocks in the Central Belt are known to be as young as Cretaceous, but given the Early or Middle Jurassic age of some of the chert, and the model of chert over basalt deposition, the possibility of Cretaceous rocks in this unit seems questionable

GREAT VALLEY COMPLEX

Great Valley Sequence

Ka **Atascadero Formation (Late Cretaceous)**—Marine, medium-bedded to very thick bedded, greenish-gray to yellowish-brown sandstone; brown- and buff-weathering, thin- and medium-bedded, medium-gray, fine-grained, biotite-rich lithic wacke; medium-brown, medium- to coarse-grained, biotite-lithic arkosic wacke; massive, medium- to coarse-grained, brown- and green-weathering, gray biotite-lithic sandstone; dark-brown and green biotite siltstone and shale; olive-gray and greenish-gray shale and mudstone. Shale and mudstone locally concretionary. Sandstone locally pebbly to cobbly. This unit has yielded a Late Cretaceous *Inoceramus* (Bivalvia; Mollusca) in the Pebblestone Shut-In quadrangle (D.L. Jones, written commun., 1985). Directly east of the map area, the Atascadero Formation has yielded many Late Cretaceous, possibly Coniacian-Maastrichtian but predominantly Campanian, fossils (Seiders, 1982), whereas in the Atascadero area the unit has fossils as old as early Late Cretaceous (Cenomanian or Turonian, Hart, 1976)

Kac **Atascadero Formation, conglomerate member**—Thick-bedded to very thick bedded pebble to cobble conglomerate. Clasts mostly felsic volcanic rocks, with subordinate intermediate to mafic volcanic, granitic, and (or) quartz sandstone clasts

KJt **Toro Formation (Early Cretaceous and Late Jurassic)**—Marine, thin-bedded, brown-weathering, dark-brown, biotite-lithic wacke; medium- to dark-gray and olive-gray mudstone; fine- to medium-grained lithic arkose; coarse-grained lithic wacke; thin-bedded, light-gray-weathering, dark-brown mudstone and siltstone. Fine-grained strata locally include orange dolomite concretions. Bedding locally rhythmic. This unit contains Early Cretaceous (Valanginian) *Buchia* (Mollusca; Bivalvia) in the map area (Seiders, 1989a), whereas directly east of the map area it includes Latest Jurassic and Early Cretaceous (Tithonian to Valanginian) fossils (Seiders, 1982)

KJtc **Toro Formation, conglomerate member**—Thick-bedded to very thick bedded pebble to boulder conglomerate. Clasts mainly chert and quartz sandstone, with subordinate granite and gabbro. Matrix is hard, dark-gray biotite-quartz-lithic sandstone

Coast Range ophiolite

Jch **Chert (Late Jurassic)**—Thin-bedded, green and gray chert, partly tuffaceous or argillaceous. Locally includes grayish-green tuff and dark-gray argillite. This unit has yielded Late Jurassic (late Tithonian) radiolarians (Seiders, 1989b)

Jo **Undifferentiated ophiolitic rocks (Middle and Late Jurassic)**—Serpentinite, diabase, diorite, and mafic volcanic rocks. U-Pb (zircon) analysis of rocks

from this unit in the Piedras Blancas block (Mattinson and Hopson, 2008) has yielded an age of 165.580±0.038 Ma

Jv **Mafic volcanic rocks**—Reddish-weathering basalt, pillow basalt, basalt breccia. Locally includes lenses of chert that have in one place yielded Late Jurassic (Tithonian) radiolarians (Seiders, 1989b), indicating that the age of parts of the ophiolite are as young as Late Jurassic

Jdb **Diabase and diorite**—Gray and greenish-gray, fine- to medium-grained

Jgb **Gabbro**—Only one body near the east edge of the map area on Santa Rosa Creek mapped separately

Jsp **Serpentinite**—Green and blue-green, massive to completely sheared serpentinite and serpentinized ultramafic rocks. Locally includes blue-gray serpentinite schist. Most ultramafic rocks are completely serpentinized (bastite), but the interior of the large body at Burro Mountain is relatively unaltered (Loney and others, 1971)

References Cited

Addicott, W.O., 1976, Neogene chronostratigraphy of nearshore marine basins of the eastern North Pacific: Proceedings of the First International Congress on Pacific Neogene Stratigraphy, p. 151–175.

Addicott, W.O., 1979, Oligocene molluscan biostratigraphy of The Indians, Santa Lucia Range, Central California, *in* Graham, S.A., ed., Tertiary and Quaternary geology of the Salinas Valley and Santa Lucia Range, Monterey County, California: Society of Economic Paleontologists and Mineralogists, Pacific Section, Pacific Coast Paleogeography Field Guide 4, p. 45–50.

Baranov, V.I., 1957, A new method for interpretation of aeromagnetic maps—Pseudo-gravimetric anomalies: Geophysics, v. 22, p. 359–383.

Barbeau, D.L., Jr., Ducea, M.N., Gehrels, G.E., Kidder, Steven, Wetmore, P.H., and Saleeby, J.B., 2005, U-Pb detrital-zircon geochronology of northern Salinian basement and cover rocks: Geological Society of America Bulletin, v. 117, no. 3–4, p. 466–481.

Barth, A.P., Wooden, J.L., Grove, Marty, Jacobsen, C.E., and Pedrick, J.N., 2003, U-Pb geochronology of rocks in the Salinas Valley region of California—A reevaluation of the crustal structure and origin of the Salinian block: Geology, v. 31, p. 517–520.

Berkland, J.O., 1973, Rice Valley outlier—New sequence of Cretaceous-Paleocene strata in the northern Coast Ranges, California: Geological Society of America Bulletin, v. 84, p. 2389–2406.

Blake, G.H., 1981, Biostratigraphic relationship of Neogene benthic foraminifera from the southern California outer continental borderland to the Monterey Formation *in* Garrison, R.E., and Douglas, R.G., eds., The Monterey Formation and related siliceous rocks of California: Los Angeles, California, Society Economic Paleontologists and Mineralogists, Pacific Section, p. 1–14.

Blake, G.H., 1991, Review of the Neogene biostratigraphy and stratigraphy of the Los Angeles Basin and implications for basin evolution, *in* Biddle, K.T., ed., Active Margin Basins: Tulsa, Oklahoma, American Association of Petroleum Geologists, p. 135–184.

Blake, M.C., Jr., Graymer, R.W., and Stamski, R.E., 2002, Geologic map and map database of western Sonoma, northernmost Marin, and southernmost Mendocino Counties, California:

U.S. Geological Survey Miscellaneous Field Studies Map MF–2402, 45 p., 1 sheet, scale 1:100,000, 11 Arc/Info coverages. (Available at http://pubs.usgs.gov/mf/2002/2402/.)
Blake, M.C., Jr., Howell, D.G., and Jones, D.L., 1982, Preliminary tectonostratigraphic terrane map of California: U.S. Geological Survey Open-File Report 82–593, 9 p., 5 plates.
Blake, M.C., Jr, Jayko, A.S., Murchey, B.L., and Jones, D.L., 1992, Formation and deformation of the Coast Range Ophiolite and related rocks near Paskenta, California: American Association of Petroleum Geologists Bulletin, v. 76, no. 3, p. 417.
Blake, M.C., Jr., and Jones, D.L., 1974, Origin of Franciscan mélanges in northern California: Society of Economic Paleontologists and Mineralogists, Special Paper No. 19, p. 255–263.
Blakely, R.J., 1995, Potential theory in gravity and magnetic applications: Cambridge, England, Cambridge University Press, 441 p.
Blakely, R.J., and Simpson, R.W., 1986, Approximating edges of source bodies from magnetic or gravity anomalies: Geophysics, v. 51, p. 1494–1498.
Buckley, S.L., 1986, Geochemistry of the Morro Rock-Islay Hill intrusive complex, San Luis Obispo County, California: Los Angeles, California State University, M.S. thesis, 66 p.
Burch, S.H., 1968, Tectonic emplacement of the Burro Mountain ultramafic body, Santa Lucia Range, California: Geological Society of America Bulletin, v. 79, p. 527–544.
Burch, S.H., Grannell, R.B., and Hanna, W.F., 1971, Bouguer gravity map of California, San Luis Obispo sheet: California Division of Mines and Geology, scale 1:250,000.
Butler, P.J., 1984, Upper Cretaceous turbidites, southwest Monterey County, California: Stanford, California, Stanford University, M.S. thesis, 67 p.
California Division of Oil, Gas, and Geothermal Resources, 1982, Oil and gas prospect wells drilled in California through 1980: California Division of Oil, Gas, and Geothermal Resources Report TR01, 258 p.
California Seismic Safety Commission, 2004, Findings and recommendations from the San Simeon earthquake of December 22, 2003: California Seismic Safety Commission Publication, no. 04-02, 10 p.
CDMG (California Division of Mines and Geology), 1986a, Official map of Alquist-Priolo Earthquake Fault Hazard Zones, Burro Mountain Quadrangle: California Division of Mines and Geology, scale 1:24,000.
CDMG (California Division of Mines and Geology), 1986b, Official map of Alquist-Priolo Earthquake Fault Hazard Zones, Piedras Blancas Quadrangle: California Division of Mines and Geology, scale 1:24,000.
CDMG (California Division of Mines and Geology), 1986c, Official map of Alquist-Priolo Earthquake Fault Hazard Zones, San Simeon Quadrangle: California Division of Mines and Geology, scale 1:24,000.
Clark, J.C., Brabb, E.E., Greene, H.G., and Ross, D.C., 1984, Geology of Point Reyes Peninsula and implications for San Gregorio Fault history *in* Crouch, J.K., and Bachman, S.B., eds., Tectonics and sedimentation along the California margin: Society of Economic Paleontologists and Mineralogists, Pacific Section, v. 38, p. 67–85.
Cole, R.B., and Stanley, R.G., 1998, Volcanic rocks of the Santa Maria province, California: U.S. Geological Survey Bulletin 1995–R, p. R1–R35.
Compton, R.R., 1960, Charnockitic rocks of Santa Lucia Range, California: American Journal of Science, v. 258, no. 9, p. 609–636.
Cordell, Lindrith, and Grauch, V.J.S., 1985, Mapping basement magnetization zones from aeromagnetic data in the San Juan Basin, New Mexico, *in* Hinze, W.J., ed., The utility of

regional gravity and magnetic anomaly maps: Society of Exploration Geophysicists, p. 181–192.
Decade of North American Geology Project, 1987, Gravity anomaly map of North America: Geological Society of America Map 2, scale 1:5,000,000.
DeMets, Charles, Gordon, R.G., and Argus, D.F., 2010, Geologically current plate motions: Geophysical Journal International, v. 181, issue 1, p. 1–80.
Dibblee, T.W., 1971, Geologic maps of seventeen 15-minute quadrangles (1:62,500) along the San Andreas Fault in vicinity of King City, Coalinga, Panoche Valley, and Paso Robles, California, with index map: U.S. Geological Survey, Open-File Report OF-71-87, scale 1:62,500.
Dibblee, T.W., Jr., 1976, The Rinconada and related faults in the southern Coast Ranges, California, and their tectonic significance: U.S. Geological Survey Professional Paper 981, 61 p.
Dibblee, T.W., Jr., and Nilsen, T.H., 1977, Lower Tertiary stratigraphy from the Ponoche Creek area to Domengine Creek area and Vallecitos area, California, *in* Payne, Max, ed., The Paleogene of the Panoche Creek-Cantua Creek area, central California: Society of Economic Paleontologists and Mineralogists, Pacific Section, p. 28–37.
Dickinson, W.R., 1971, Clastic sedimentary sequences deposited in shelf, slope, and trough settings between magmatic arcs and associated trenches: Pacific Geology, v. 3, p. 15–30.
Dickinson, W.R., 1983, Cretaceous sinistral strike slip along Nacimiento Fault in Coastal California: American Association of Petroleum Geologists Bulletin, v. 67, no. 4, p. 624–645.
Dickinson, W.R., Ducea, Mihai, Rosenberg, L.I., Green, H.G., Graham, S.A., Clark, J.C., Weber, G.E., Kidder, Steven, Ernst, W.G., and Brabb, E.E., 2005, Net dextral slip, Neogene San Gregorio-Hosgri Fault Zone, Coastal California—Geologic evidence and tectonic implications: Geological Society of America Special Paper 391, 43 p.
Dickinson, W.R., Hopson, C.A., Saleeby, J.B., Schweickert, R.A., Ingersoll, R.V., Pessagno, E.A., Jr., Mattinson, J.M., Luyendyk, B.P., Beebe, Ward, Hull, D.M., Munoz, I.M., and Blome, C.D., 1996, Alternate origins of the Coast Range Ophiolite (California); introduction and implications: GSA Today, v. 6, no. 2, p. 1–10.
Douglas, R.G., 1981, Paleoecology of continental margin basins—A modern case history from the borderland of southern California, *in* Douglas, R.G., ed., Depositional systems of active continental margin basins, Short Course Notes: Society of Economic Paleontologists and Mineralogists, Pacific Section, p. 121–156.
Ducea, M.N., Kidder, Steven, Chesley, J.T., and Saleeby, J.B., 2009, Tectonic underplating of trench sediments beneath magmatic arcs—The central California example: International Geology Review, v. 51, no. 1, p. 1–26.
Ducea, M.N., Kidder, Steven, and Zandt, George, 2003, Arc composition at mid-crustal depths—Insights from the Coast Ridge belt, Santa Lucia Mountains, California: Geophysical Research Letters, v. 30, 1703, doi:10.1029/2002GL016297.
Durham, D.L., 1965, Geology of the Jolon and Williams Hill quadrangles, Monterey County, California: U.S. Geological Survey Bulletin B–1181–Q, p. 1–27.
Durham, D.L., 1968, Geology of the Tierra Redonda and Bradley quadrangles, Monterey and San Luis Obispo counties, California: U.S. Geological Survey Bulletin 1255, scale 1:24,000.
Durham, D.L., 1974, Geology of the southern Salinas Valley area, California: U.S. Geological Survey Professional Paper 819, 106 p., 4 pls.

Ernst, W.G., and Hall, C.A., Jr., 1974, Geology and petrology of the Cambria Felsite, a new Oligocene formation, west-central California Coast Ranges: Geological Society of America Bulletin, v. 85, p. 523–532.
Ernst, W.G., Martens, U.C., McLaughlin, R.J., Clark, J.C., and Moore, D.E., 2011, Zircon U-Pb age of the Pescadero felsite—A Late Cretaceous igneous event in the forearc, west-central California Coast Ranges: Geological Society of America Bulletin, doi:10.1130/B30270.1.
Gilbert, W.G., 1971, Sur fault zone, Monterey County, California: Stanford, California, Stanford University, Ph.D. thesis, 160 p.
Graham, S.A., 1978, Role of Salinian block in evolution of San Andreas Fault system, California: American Association of Petroleum Geologists Bulletin, v. 62, p. 2214–2231.
Graham, S.A., 1979, Tertiary stratigraphy and depositional environments near Indians Ranch, Monterey County, California, *in* Graham, S.A., ed., Tertiary and Quaternary geology of the Salinas Valley and Santa Lucia Range, Monterey County, California: Society of Economic Paleontologists and Mineralogists, Pacific Section, Pacific Coast Paleogeography Field Guide 4, p. 3–12.
Graham, S.A., and Dickinson, W.R., 1978, Evidence for 115 kilometers of right slip on the San Gregorio-Hosgri fault trend: Science, v. 199, p. 179–181.
Graham, S.A., Seedorf, D.C., Walter, O., and Bloch, R.B., 1991, San Andreas Fault to Pacific Coast, *in* West coast regional cross section: American Association of Petroleum Geologists, sheet 2 of 3.
Grauch, V.J.S., and Cordell, Lindrith, 1987, Limitations of determining density or magnetic boundaries from the horizontal gradient of gravity or pseudogravity data: Geophysics, v. 52, no. 1, p. 118–121.
Graymer, R.W., 2005, Jurassic-Cretaceous assembly of central California, *in* Stevens, Calvin, and Cooper, John, eds., Mesozoic tectonic assembly of California: Society of Economic Paleontologists and Mineralogists, Pacific Section, book 96, p. 21–64.
Graymer, R.W., Langenheim, V.E., Rosenberg, L.I., Colgan, J.P., and Roberts, M.A., 2010, New insights into the tectonics of the central California Coast Ranges from cross sections based on digital geologic mapping and potential-field geophysics [abs.]: Geological Society of America Abstracts with Programs, v. 42, no. 4, p. 82.
Grove, K., 1993, Latest Cretaceous basin formation within the Salinian terrane of west-central California: Geological Society of America Bulletin, v. 105, p. 447–463.
Hagstrum, J.T., 1997, Paleomagnetism, paleogeographic origins, and remagnetization of the Coast Range ophiolite and Great Valley Sequence, Alta and Baja California: American Association of Petroleum Geologists Bulletin, v. 81, no. 4, p. 686–687.
Hall, C.A., 1974, Geologic map of the Cambria region, San Luis Obispo County, California: U.S. Geological Survey Miscellaneous Field Studies Map MF–599, 2 sheets, scale 1:24,000.
Hall, C.A., Jr., 1975, San Simeon-Hosgri Fault System, coastal California—Economic and environmental implications: Science, v. 190, no. 4221, p. 1291–1294.
Hall, C.A., 1976, Geologic map of the San Simeon-Piedras Blancas region, San Luis Obispo County, California: U.S. Geological Survey Miscellaneous Field Studies Map MF–784, 1 sheet, scale 1:24,000.
Hall, C.A., Jr., 1991, Geology of the Point Sur-Lopez Point region, Coast Ranges, California—A part of the Southern California allochthon: Geological Society of America Special Paper, v. 266, 40 p., 2 plates.

Hall, C.A., Jr., Ernst, W.G., Prior, S.W., and Weise, J.W., 1979, Geological map of the San Luis Obispo-San Simeon region, California: U.S. Geological Survey Miscellaneous Investigations Series Map I–1097, scale 1:48,000.

Hall, C.A., Jr., Turner, D.L., and Surdam, R.C., 1966, Potassium–argon age of the Obispo Formation with *Pecten lompocensis Arnold*, southern Coast Ranges, California: Geological Society of America Bulletin, v. 77, no. 4, p. 443–446.

Hamilton, Warren, 1978, Mesozoic tectonics of the western United States, *in* Howell, D.G., and McDougall, K.A., eds., Mesozoic Paleogeography of the Western United States: Society of Economic Paleontologists and Mineralogists, p. 33–70.

Hanson, K., Wesling, J., Lettis, W., Kelson, K., and Metzger, L., 1994, Correlation, ages, and uplift rates of Quaternary marine terraces, south central coastal California, *in* Altermann I., McMullen, R., Cluff, L., and Slemmons, D., eds., Seismotectonics of the central California Coast Ranges: Boulder, Geological Society of America Special Paper 292, p. 45–71.

Hardebeck, J.L., 2010, Seismotectonics and fault structure of the California central Coast Ranges: Bulletin of the Seismological Society of America, v. 100, p. 1031–1050.

Harms, T.A., Jayko, A.S., and Blake, M.C., Jr., 1992, Kinematic evidence for extensional unroofing of the Franciscan Complex along the Coast Range Fault, northern Diablo Range, California: Tectonics, v. 11, p. 228–241.

Hart, E.W., 1976, Basic geology of the Santa Margarita area, San Luis Obispo County, California: California Division of Mines and Geology Bulletin, no. 199, 45 p., scale 1:24,000.

Heiskanen, W.A., and Vening-Meinesz, F.A., 1958, The Earth and its gravity field: New York, McGraw-Hill Book Company, Inc., 470 p.

Hill, M.L., and Dibblee, T.W., Jr., 1953, San Andreas, Garlock, and Big Pine Faults, California—A study of the character, history, and tectonic significance of their displacements: Geological Society of America Bulletin, v. 64, p. 443–458.

Hoffman, Jonathan, Prothero, D.R., and Donohoo, L.L., 2001, Magnetic stratigraphy of the Oligocene-Miocene Vaqueros Formation and molluscan stage, California: Geological Society of America Abstracts with Programs, v. 33, no. 3, p. 60.

Hopson, C.A., Mattinson, J.M., Luyendyk, B.P., Beebe, W.J., Pessagno, E.A., Jr., Hull, D.M., Munoz, I.M., and Blome, C.D., 1997, Coast Range ophiolite—Paleoequatorial ocean-ridge lithosphere: American Association of Petroleum Geologists Bulletin, v. 81, no. 4, p. 687.

Howell, D.G., Vedder, J.G., McLean, Hugh, Joyce, J.M., Clarke, S.H., Jr., and Smith, Greg, 1977, Review of Cretaceous geology, Salinian and Nacimiento blocks, Coast Ranges of central California, *in* Howell, D.G., Vedder, J.G., and McDougall, K., Cretaceous geology of the California Coast Ranges west of the San Andreas Fault: Society of Economic Paleontologists and Mineralogists, The Pacific Section, Pacific Coast Paleogeography Field Guide, no. 2, p. 1–46.

Howie, J.M., Miller, K.C., and Savage, W.U., 1993, Integrated crustal structure across the south-central California margin—Santa Lucia escarpment to the San Andreas Fault: Journal of Geophysical Research, v. 98, p. 8173–8196.

Hsu, K.J., 1969, Preliminary report and geologic guide to Franciscan mélanges of the Morro Bay-San Simeon area, California: California Division of Mines and Geology Special Publication, no. 35, 46 p.

Ingle, J.C., Jr., 1980, Cenozoic paleobathymetry and depositional history of selected sequences within the southern California Borderland: Cushman Foundation for Foraminiferal Research, Special Publication, no. 19, p. 163–195.

Ingle, J.C., Jr., and Keller, G., 1980, Benthic foraminiferal biofacies of the eastern Pacific margin between 40° S and 32° N *in* Field, M.E., Douglas, R.G. and others, eds., Quaternary depositional environments of the Pacific Coast: Society of Economic Paleontologists and Mineralogists, Pacific Section, p. 341–355.

Jachens, R.C., and Griscom, Andrew, 1985, An isostatic residual gravity map of California—A residual map for interpretation of anomalies from intracrustal sources, *in* Hinze, W.J., ed., The utility of regional gravity and magnetic maps: Society of Exploration Geophysicists, p. 347–360.

Jachens, R.C., Langenheim, V.E., Wentworth, C.M., Simpson, R.W., and Graymer, R.W., 2009, Defining fault offsets from aeromagnetic anomalies, central California Coast Ranges: Geological Society of America Abstracts with Programs, v. 41, no. 7, p. 281.

Jachens, R.C., Wentworth, C.M., and McLaughlin, R.J., 1998, Pre-San Andreas location of the Gualala block inferred from magnetic and gravity anomalies, *in* Elder, W.P., ed., Geology and tectonics of the Gualala block, northern California: Society of Economic Paleontologists and Mineralogists, Pacific Section, book 84, p.27–64.

Jacobson, C.E., Grove, M., Pedrick, J.N., Barth, A.P., Marsaglia, K.M., Gehrels, G.E., and Nourse, J.A., 2011, Late Cretaceous-early Cenozoic tectonic evolution of the southern California margin inferred from provenance of trench and forearc sediments: Geological Society of America Bulletin, v. 123, p. 485–506.

Kelley, F.R., comp., 1982, Thermal springs and wells and radiometric ages of rocks in the Santa Rosa quadrangle, California, *in* Wagner, D.L., and Bortugno, E.J., comps., Geologic map of the Santa Rosa quadrangle, California: California Division of Mines and Geology Regional Map Series, map no. 2A, sheet 4, 28 p., scale 1:250,000.

Kidder, S.B., and Ducea, M.N., 2006, High temperatures and inverted metamorphism in the schist of Sierra de Salinas, California: Earth and Planetary Science Letters, v. 241, p. 422-437.

Kistler, R.W., and Champion, D.E., 2001, Rb-Sr whole-rock and mineral ages, K-Ar, $^{40}Ar/^{39}Ar$, and U-Pb mineral ages, and strontium, lead, neodymium, and oxygen isotopic compositions for granitic rocks from the Salinian composite terrane, California: U.S. Geological Survey Open-File Report 2001–0453, 80 p. (Available at http://pubs.usgs.gov/of/2001/0453).

Krueger, S.W., and Jones, D.L., 1989, Extensional fault uplift of regional Franciscan blueschists due to subduction shallowing during the Laramide Orogeny: Geology, v. 17, p. 1157–1159.

Langenheim, V.E., Jachens, R.C., Graymer, R.W., Colgan, J.P., Stanley, R.G., and Wentworth, C.M., 2013, Fault geometry and cumulative offsets in the central Coast Ranges, California—Evidence for northward increasing slip along the San Gregorio-Hosgri Fault: Lithosphere, v. 5, p. 29–48.

Langenheim, V.E., Jachens, R.C., Graymer, R.W., Wentworth, C.M., Colgan, J.P., and Stanley, R.G., 2010, Implications of cumulative offsets along the San Gregorio-Hosgri Fault, California—Why the Santa Maria Basin matters [abs.]: Geological Society of America Abstracts with Programs, v. 42, no. 4, p. 81.

Langenheim, V.E., Jachens, R.C., and Moussaoui, Khaled, 2009, Aeromagnetic survey map of the central California Coast Ranges: U.S. Geological Survey Open-File Report 2009–1044. (Available at http://pubs.usgs.gov/of/2009/1044.)

Lin, Guoqing, Thurber, C.H., Zhang, Haijiang, Hauksson, Egill, Shearer, P.M., Waldhauser, Felix, Brocher, T.M., and Hardebeck, Jeanne, 2010, A California statewide three-dimensional seismic velocity model from both absolute and differential times: Bulletin of the Seismological Society of America, v. 100, p. 225–240.

Loel, Wayne, and Corey, W.H., 1932, Paleontology, pt. 1 of The Vaqueros Formation, lower Miocene of California: California University Publications, Department of Geological Sciences Bulletin, v. 22, no. 3, p. 31–410.
Loney, R.A., Himmelberg, G.R., and Coleman, R.G., 1971, Structure and petrology of the alpine-type peridotite at Burro Mountain, California, U.S.A.: Journal of Petrology, v. 12, no. 2, p. 245–309.
Malmblorg, W.T., West, W.B., Brabb, E.E., and Parker, J.M., 2008, Digital coordinates and age of more than 13,000 foraminifer samples collected by Chevron petroleum geologists in California: U.S. Geological Survey Open-File Report, 2008–1187, 3 p., 2 database files. (Available at http://pubs.usgs.gov/of/2008/1187/.)
Matthews, Vincent, III, 1973, Pinnacles-Neenach correlation—A restriction for models of the origin of the Transverse Ranges and the Big Bend in the San Andreas Fault: Geological Society of America Bulletin, v. 84, p. 683–688.
Mattinson, J.M., 1978, Age, origin, and thermal histories of some plutonic rocks from the Salinian block of California: Contributions to Mineralogy and Petrology, v. 67, no. 3, p. 233–245.
Mattinson, J.M,, and Hopson, C.A., 2008, New high-precision CA-TIMS U/Pb zircon plateau ages for the Point Sal and San Simeon ophiolite remnants, California Coast Ranges: Geological Society of America Special Paper, v. 438, p. 103–112.
McCulloch, D.S., and Chapman, R.H., 1977, Map showing residual magnetic intensity along the California Coast, lat 37°30’ N. to lat 34°30’ N.: U.S. Geological Survey Open-File Report 77–079, 14 sheets, scale 1:125,000.
McDougall, K., 2008, California Cenozoic Biostratigraphy–Paleogene *in* Hosford Scheirer, A., ed., Petroleum systems and geologic assessment of oil and gas in the San Joaquin Basin Province, California: U.S. Geological Survey Professional Paper 1713, ch. 4, 30 p.
McLaren, M.K., Hardebeck, J.L., van der Elst, Nicholas, Unruh, J.R., Bawden, G.W., and Blair, J.L., 2008, Complex faulting associated with the 22 December 2003 M_w 6.5 San Simeon, California, earthquake, aftershocks, and postseismic deformation: Bulletin of the Seismological Society of America, v. 98, p. 1659–1680.
Morisani, A.M., Housh, T.B., Tripathy, Alka, Jacobsen, C.E., and Cloos, Mark, 2005, Detrital zircon geochronology of greywacke blocks within the Franciscan mélange at San Simeon, California—Depositional age and provenance implications [abs.]: Geological Society of America Abstracts with Programs, v. 37, no. 7, p. 18–19.
Murchey, B.M., and Jones, D.L., 1984, Age and significance of chert in the Franciscan Complex in the San Francisco Bay Region, *in* Blake, M.C., Jr., ed., Franciscan geology of northern California: Society of Economic Paleontologists and Mineralogists, Pacific Section, v. 43, p. 23–30.
Page, B.M., 1970, Sur-Nacimiento Fault zone of California—Continental margin tectonics: Geological Society of America Bulletin, v. 81, no. 3, p. 667–668
Pan-American Center for Earth and Environmental Studies, 2010, Gravity database, accessed April, 10, 2010 at http://irpsvgis00.utep.edu/repositorywebsite (Accessed July 15, 2013 at http://research.utep.edu/default.aspx?tabid=37229).
Plouff, Donald, 1977, Preliminary documentation for a FORTRAN program to compute gravity terrain corrections based on topography digitized on a geographic grid: U.S. Geological Survey Open-File Report 77–535, 45 p.

Powell, R.E., 1993, Balanced palinspastic reconstruction of pre-late Cenozoic paleogeology, southern California—Geologic and kinematic constraints on evolution of the San Andreas Fault system, *in* Powell, R.E., Weldon, R.J., and Matti, J.C., eds., The San Andreas Fault system—Displacement, palinspastic reconstruction, and geologic evolution: Geological Society of America Memoir 178, 332 p., 8 plates.

Prothero, D.R., and Donohoo, L.L, 2001, Magnetic stratigraphy of the lower Miocene (early Hemingfordian) Sespe-Vaqueros formations, Orange County, California, *in* Prothero, D.R., ed., Magnetic stratigraphy of the Pacific Coast Cenozoic: Society of Economic Paleontologists and Mineralogists, Pacific Section, , p. 242–253.

Prothero, D.R., and Hoffman, Jonathan, 2001, Magnetic stratigraphy of upper Oligocene-lower Miocene Soda Lake Shale Member of the Vaqueros Formation, Caliente Range, San Luis Obispo County, California, *in* Prothero, D.R., ed., Magnetic stratigraphy of the Pacific Coast Cenozoic: Society of Economic Paleontologists and Mineralogists, Pacific Section, p. 254–262.

Roberts, C.W., Jachens, R.C., and Oliver, H.W., 1990, Isostatic residual gravity map of California and offshore southern California: California Division of Mines and Geology, Geologic data map no. 7, scale 1:750,000.

Rockwell, T.K., Bickner, F.R., Vaughan, P.R., and Hanson, K.L., 1987, Applications of soil geomorphology to dating and correlating coastal terrace deposits across the San Simeon Fault zone, central California [abs.]: Geological Society of America Abstracts with Programs, v. 19, no. 6, p. 444.

Rosenberg, L.I., and Clark, J.C., 2009, Map of the Rinconada and Reliz Fault zones, Salinas River Valley, California: U.S. Geological Survey Scientific Investigations Map 3059, 30 p., 1 sheet.

Seiders, V.M., 1982, Geologic map of an area near York Mountain, San Luis Obispo County, California: U.S. Geological Survey Miscellaneous Investigations Series I–1369, 1 sheet, scale 1:24,000.

Seiders, V.M., 1989a, Geologic map of the Burnett Peak quadrangle, Monterey and San Luis Obispo counties, California: U.S. Geological Survey Geologic Quadrangle Map GQ–1658, 1 sheet, scale 1:24,000.

Seiders, V.M, 1989b, Geologic map of the Burro Mountain quadrangle, Monterey and San Luis Obispo counties, California: U.S. Geological Survey Miscellaneous Field Studies Map MF–2090, 1 sheet, scale 1:24,000.

Seiders, V.M., Joyce, J.M., Leverett, K.A., and McLean, Hugh, 1983, Geologic map of part of the Ventana Wilderness and the Black Butte, Bear Mountain, and Bear Canyon roadless areas, Monterey County, California: U.S. Geological Survey Miscellaneous Field Studies Map MF–1559–B, scale 1:50,000.

Smith, G.W., 1978, Stratigraphy, sedimentology, and petrology of the Cambria Slab, San Luis Obispo County, California: Albuquerque, University of New Mexico, M.S. thesis, 123 p.

Sorlien, C.C., Kamerling, M.J., and Mayerson, Drew, 1999, Block rotation and termination of the Hosgri strike-slip fault, California, from three-dimensional map restoration: Geology, v. 27, p. 1039–1042.

Stanley, R.G., Johnson, S.Y., Obradovich, J.D., Tuttle, M.L., Thornton, M.L., Vork, D.R., Filewicz, M.V., Mason, M.A., Swisher, C.C., III, 1990, Age and depositional setting of the type Lospe Formation (lower Miocene), Santa Maria Basin, central California [abs.]: American Association of Petroleum Geologists Bulletin, v. 74, no. 5, p. 770–771.

Stanley, R.G., Johnson, S.Y., Swisher, C.C., III, Mason, M.A., Obradovich, J.D., Cotton, M.L., Filewicz, M.V. and Vork, D.R., 1996, Age of the Lospe Formation (early Miocene) and origin of the Santa Maria basin, California: U.S. Geological Survey Bulletin 1995–M, 37 p.

Stierman, D.J., and Kovach, R.L., 1979, An in situ velocity study—The Stone Canyon well: Journal of Geophysical Research, v. 84, no. B2, p. 672–678.

Telford, W.M., Geldart, L.O., Sheriff, R.E., and Keyes, D.A., 1976, Applied Geophysics: New York, Cambridge University Press, 960 p.

Turner, D.L., 1968, Potassium–argon dates concerning the Tertiary foraminiferal time scale and San Andreas Fault displacement: Berkeley, University of California, Ph.D. dissertation, 99 p.

Underwood, M.B., and Laughland, M.B., 2001, Paleothermal structure of the Point San Luis slab of central California—Effects of Late Cretaceous underplating, out-of-sequence thrusting, and late Cenozoic dextral offset: Tectonics, v. 20, p. 97–111.

Underwood, M.B., Laughland, M.B., Shelton, K.L., and Sedlock, R.L., 1995, Thermal-maturity trends within Franciscan rocks near Big Sur, California—Implications for offset along the San Gregorio-San Simeon-Hosgri fault zone: Geology, v. 23, p. 839–842.

U.S. Geological Survey, 2005, Seven aeromagnetic surveys in California and Nevada—A web site for distribution of data: U.S. Geological Survey Open-File Report 2005–1328, last accessed Feb. 2, 2011, at http://pubs.usgs.gov/of/2005/1328/ca-nev.html.

van Morkhoven, F.P.C.M., Berggren, W.A., and Edwards, A.S., 1986, Cenozoic cosmopolitan deep-water benthic foraminifera: Bulletin des Centres de Recherches Exploration-Production Elf-Aquitaine, Memoire, v. 11, 421 p.

Weber, G.E., 1983, Geological investigation of the marine terraces of the San Simeon region and Pleistocene activity on the San Simeon Fault zone, San Luis Obispo County, California: Menlo Park, California, unpublished technical report to U.S. Geological Survey under Contract 14-08-00001-18230, 66 p.